

THE EVALUATION OF RF CHANNEL IMPAIRMENTS
AND CO-CHANNEL INTERFERENCE
OVER Rician FADING CHANNEL

by

Zhaoheng Luo

Presented to the Faculty of the Graduate School of
The University of Texas at Arlington in Partial Fulfillment
of the Requirements
for the Degree of

MASTER OF SCIENCE IN ELECTRICAL ENGINEERING

THE UNIVERSITY OF TEXAS AT ARLINGTON

December 2014

Copyright © by Zhaoheng Luo

All Rights Reserved



Acknowledgements

I am very thankful for the people who guided me and encouraged me through this research. I would like to thank my family and friends for their support.

Particularly, I would like to thank my supervising professor Dr. Qilian Liang for his guidance and patience to me throughout the whole process of research. His broad knowledge and experience in the field of wireless communication had been very useful to me and I have learned a lot from him.

I would also like to thank Dr. W. Alan Davis and Dr. Saibun Tjautja for taking the time to read my thesis and being the committee of my thesis defense.

Furthermore, I would like to thank my lab mates for giving me advice and support throughout the time of my research.

August 26, 2014

Abstract

THE EVALUATION OF RF CHANNEL IMPAIRMENTS
AND CO-CHANNEL INTERFERENCE
OVER Rician FADING CHANNEL

Zhaoheng Luo, M.S

The University of Texas at Arlington, 2014

Supervising Professor: Qilian Liang

The mobile network system has evolved into its 4th generation and the demand of faster data rate, higher network coverage and reliable communication has never stopped. In order to have more bandwidth and reduce power consumption, more and more new transmitting and receiving devices have been developed to achieve the goal. However, during this evolution, the performance of the system is suffering from effects by the radio-frequency (RF) circuit design, which produces DC offset, in-phase and quadrature (IQ) imbalance and phase noise. Also, in cellular mobile communication systems, signals from different sources can be using the same frequency spectrum, and those signals will distort each other, by producing co-channel interference (CCI) in the system.

In this thesis, the influences by each one of these interference in the Rician fading channel wireless system with QPSK modulation have been evaluated. Simulations are designed to find out the dB loss between the original system that has not interfered and the system that are affected by channel impairments and channel interference. The simulation results show that MIMO system does not suffer much from that the DC offset but the SISO system is significantly influenced. The IQ imbalance and phase noise have very little impact on both SISO and MIMO wireless systems. However, the CCI could make as large as 6.6 dB to SISO system and around 2.3 dB to MIMO system. The combined

interference, which means adding all these interference factors to the system at the same time, causes large dB loss to MIMO and SISO system, particularly when CCI has small SIR value. In most cases, MIMO system has less dB loss than SISO system when experiencing channel impairments and channel interference.

Table of Contents

Acknowledgements	iii
Abstract	iv
List of Illustrations	viii
List of Tables	x
Chapter 1 Introduction to Wireless Communication System	1
1.1 Introduction	1
1.2 Organization of the thesis	2
Chapter 2 Wireless Communication System Model	3
2.1 Introduction	3
2.2 Wireless communication System Model	4
Information bits	4
Burst Builder	4
Modulation	5
Up sampling	5
Pulse shaping filter	5
Rician fading Channel	5
Matched Filter	6
Down Sampling	6
Channel estimation	6
Demodulation	6
Burst Extractor	6
2.3 Wireless Channel Model	7
1. Long-term fading due to path loss and shadowing	7
2. Short-term fading due to multipath and mobility	7

2.4 Multiple Input Multiple Output (MIMO) technology	9
2.5 Alamouti Code	12
2.6 Channel Estimation Model.....	14
Chapter 3 Radio Frequency (RF) Channel Impairments	19
3.1 Introduction	19
3.2 DC Offset Model	20
3.3 DC Offset Simulation Results	23
3.4 IQ Imbalance model	26
3.5 IQ Imbalance Simulation Results	28
3.6 Phase Noise Model	31
3.7 Phase Noise Simulation Results	34
Chapter 4 Co-Channel Interferences	38
4.1 Introduction	38
4.2 Co-Channel Interference System Model	39
4.3 Co-Channel Interference Simulation Results	42
Chapter 5 Combined Interference.....	49
5.1 Introduction	49
5.2 Combined Interference System Model	49
5.3 Combined Interference Simulation Results	51
Chapter 6 Conclusion and Future Work.....	54
6.1 Conclusion	54
6.2 Future Work	57
References	58
Biographical Information	60

List of Illustrations

Figure 2-1 Wireless Communication System Block Diagram	4
Figure 2-2 Rician Distribution Probability Distribution Histogram	9
Figure 2-3 Optimal Tradeoff Between Spatial Multiplexing Gain And Diversity Gain	11
Figure 2-4 Space Time Coding Communication System Block Diagram	11
Figure 2-5 2x2 Alamouti Space-Time Block Code Antennas.....	12
Figure 2-6 QPSK Modulation Symbols	15
Figure 2-7 Symbols with AWGN noise.....	15
Figure 3-1 DC Offset Interference Block Diagram	21
Figure 3-2 Modulated Symbol.....	22
Figure 3-3 Symbols with DC Offset Interference	22
Figure 3-4 DC Offset BER Performance for $k = 7$ dB, $f_d = 20$ Hz.....	23
Figure 3-5 DC Offset BER Performance for $k = 12$ dB, $f_d = 100$ Hz	24
Figure 3-6 DC Offset BER Performance for $k = 200$ dB, $f_d = 0$ Hz	25
Figure 3-7 IQ Imbalance Interference Block Diagram	27
Figure 3-8 Modulated Symbols	27
Figure 3-9 Symbols with IQ Imbalance	28
Figure 3-10 IQ Imbalance BER Performance for $k = 7$ dB, $f_d = 20$ Hz.....	29
Figure 3-11 IQ Imbalance BER Performance for $k = 12$ dB, $f_d = 100$ Hz	30
Figure 3-12 IQ Imbalance BER Performance for $k = 200$ dB, $f_d = 0$ Hz.....	31
Figure 3-13 Phase Noise Interference System Diagram	32
Figure 3-14 Modulated Symbols	33
Figure 3-15 Symbols with Phase Noise	33
Figure 3-16 Phase Noise BER Performance for $k = 7$ dB, $f_d = 20$ Hz.....	35
Figure 3-17 Phase Noise BER Performance for $k = 12$ dB, $f_d = 20$ Hz.....	36

Figure 3-18 Phase noise BER Performance for $k = 200$ dB, $fd = 0$ Hz	37
Figure 4-1 Co-Channel Interference in MIMO System	38
Figure 4-2 Co-Channel Interference System Block Diagram.....	40
Figure 4-3 Modulated Symbols	40
Figure 4-4 Symbols with Co-Channel Interference.....	41
Figure 4-5 CCI BER Performance for $k = 7$ dB, $fd = 20$ Hz.....	43
Figure 4-6 CCI BER Performance for $k = 12$ dB, $fd = 100$ Hz.....	45
Figure 4-7 CCI BER Performance for $k = 200$ dB, $fd= 0$ Hz.....	47
Figure 5-1 Modulated Symbol.....	50
Figure 5-2 Symbols with Combine Interferences	50
Figure 5-3 Combined Interference BER Performance for $k = 7$ dB, $fd = 20$ Hz.....	51
Figure 5-4 Combined Interference BER Performance for $k = 12$ dB, $fd = 100$ Hz.....	52
Figure 5-5 Combined Interference BER Performance for $k = 200$ dB, $fd = 0$ Hz	53

List of Tables

Table 6-1 Summary of SISO Performance with Different Interferences	55
Table 6-2 Summary of MIMO Performance with Different Interferences.....	55

Chapter 1

Introduction to Wireless Communication System

1.1 Introduction

Wireless communications network has been one of the most explosive growing industries since the mid-1990s. It has evolved from a cutting edge technology owned by military, to an essential part of the cellular phone system that are used by billions of subscribers. In the past ten years, the evolution of mobile network continued to grow. As the 4th Generation (4G) Long term evolution (LTE) released in the year of 2008, the desire to achieve higher data rates, larger coverage areas and more reliable communications had been driving thousands of scientists and engineers to find new resolutions for better performance, in order to satisfy the high demand of reliability with wireless network system[1][2].

In modern wireless communications, due to the development of transmitting and receiving devices in order to satisfy higher bandwidth and lower power consumption, the error rate of data has been suffering from impacts by the radio-frequency (RF) circuit design, which produces DC offsets, IQ imbalance and Phase noise in the system [3]. Also, in cellular mobile communication system, signals in the same frequency are sometimes re-used, which caused co-channel interference (CCI) in the system [4]. The receivers not only pick up signals from the same cell but also signals from cells far away that are using the same frequency bands, which distorted the received signals in the system. All these undesirable factors are making negative impacts to the reliability of the wireless communication system. Evaluations of all these effects by each interferences are needed to help system engineers to decide whether or not to use compensation and cancellation schemes to improve system performance.

1.2 Organization of the thesis

This thesis has six main sections. Chapter 1 introduces the current state of development of wireless communication system. Chapter 2 explains the wireless communication system as a whole and how each part contributes to the system. It also elaborates on the channel model and MIMO system that are used for simulation. At last it explains the channel estimation method theory. Chapter 3 and 4 have similar structures. Chapter 3 introduce the impact of channel impairments to SISO and MIMO wireless system. Then it explains how each channel impairment is generated and added to the system. At last it shows and evaluates each of the channel impairment performance results. Chapter 4 introduce Co-Channel interference (CCI) first. Then explains how CCI is generated and added to the system, follow by simulation results for the system performances for SISO and MIMO. Chapter 5 evaluates the system performances if all the channel impairments and CCI are added to the system. Chapter 6 summarizes and evaluates all the simulation results, and also points out the possible solution to these interference problems.

Chapter 2

Wireless Communication System Model

2.1 Introduction

Wireless communication system is a system that transfers information from one point to another without a wires. It is widely used in the application of cordless phones, wireless local area networks, broadband wireless access, satellite networks, etc. In order to fulfill the requirement for various wireless communication systems, often use a small portion of the frequency spectrum to transfer mass data through a dynamic environment. The signal in the received end often suffer with variations by path Loss and shadowing, where transmitter power dissipated and signal attenuated by buildings and blocks in the space. The variations of the propagation of signal also change from time and affected by noise and interference.

Wireless communication system contains several key sections to convey information digitally from one place to the other. Similar to wired digital communication, channel coding, modulations and pulse shaping are used in the transmitting end before going through the wireless channel. At the receiver end, techniques for channel estimation, demodulation and channel decoding are also applied to the system to restore the original data. However, wireless communication signals are propagated through a wireless medium instead of wires. It is often not easy to obtain accurate a channel model due to the complexity of the radio channel, therefore statistical model are used in most of wireless channel modeling. [1][2]

In this thesis, it is assumed that the wireless communication system has the basic encoding and decoding process. Signals propagate through different paths to reach destinations, and they all cause the received signal to have spatially and temporally varying energy pattern (called fading). Furthermore, telecommunication engineers use channel

estimation algorithms to mitigate fading effects according to specific channel characteristics.

2.2 Wireless communication System Model

The system simulation model is illustrated in Figure 2-1 following with brief explanations of each block.

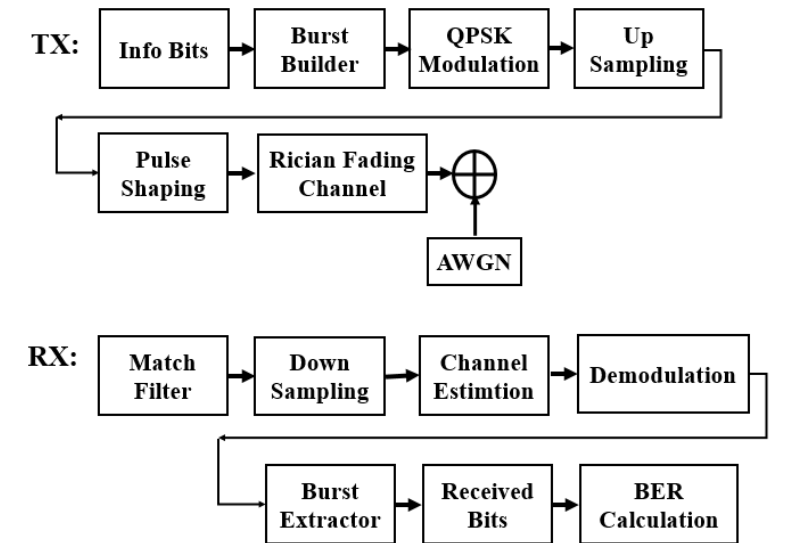


Figure 2-1 Wireless Communication System Block Diagram

Information bits: In a digital communication system, the source information is converted into a sequence of binary digits, hence the source output is a digital signal consists of randomly generated 0s and 1s. In this case we generate 10000 bits as the payload. And they are going into the burst builder.

Burst Builder: Add 3 symbols (1symbol=2bits) of guard symbols and 48 symbols of unique words to the beginning of the original message bits. The unique words are a known sequence of bits used to help synchronizations and channel estimations in this cases. The sequence of 00,01,10,11 is used as unique word for QPSK modulation in the system.

Modulation: In order to transmit a binary sequence across the wireless channel, specific signals are used to map digital sequence. In this thesis, the effect of Quadrature PSK (QPSK) modulation is studied. The phase of the carrier is varied to represent different signal elements. QPSK modulation uses 2 bits at a time and four different phases of signals to represent them. In this case,

$$00 \rightarrow 1, 01 \rightarrow j, 11 \rightarrow -1, 10 \rightarrow -j. [8]$$

Up sampling: In this case fifteen zeroes are added between each symbols. When signals are transmitted through channel with noise, fading and interference, all these effects can be reduced. The transitions between each symbols become smoother.

Pulse shaping filter: Changing the shapes and waveform of the pulses allow transmitted signals to be less affected by inter-symbol interferences (ISI). In the channel, signal characteristics such as amplitude, frequency and phase can be changed. The pulse shaping filter can help to smooth out these effects. A raised cosine filter is used as a pulsed shaping filter in this simulation. The roll off factor with range between 0 and 1, is used to represent the excess bandwidth of the filter. Let the length of the Raised Cosine Filter be N and so the output of the pulse shaping will be the $(\text{length of the burst structure}) \times 16 + N - 1$. Since only $(\text{The length of burst structure}) \times 16$ symbols are needed so $(N-1)/2$ symbols are removed at the beginning and the end of the sequence to keep length of symbols consistent with the length of the symbols before this process. The roll-off factor is 0.35 in this thesis.

Rician fading Channel: For wireless fading channel, Jake's model[5] is used for simulation. The ratio between the power in the direct path and the rest of the path is K , and f_d is used to represent the Doppler shift of the channel.

In this thesis, 3 scenarios are used for different Rician fading:

$$K=7 \text{ dB}, f_d=20 \text{ Hz}$$

$K=12$ dB, $f_d=100$ Hz

$K=200$ dB, $f_d=0$ Hz

In all the channels, additive white Gaussian noises (AWGN) are also added. The power ratio between the signal and noise is called signal to noise ratio (SNR), in the unit of dB. The complex noises (Since the signals are complex in the simulation) serve as contaminations to the wireless channels.

Matched Filter: similar to Pulse shaping filter, matched filter is used to make the signals smoother and to remove some noises. The roll-off factor is 0.35. After filtering, $(N-1)/2$ symbols are removed at the beginning and the end of the sequences.

Down Sampling: opposite to Up Sampling, down sampling removes all the zeros between the symbols. After down sampling the length of symbols should be the same as the length of the burst.

Channel estimation: An algorithm is used to detect the original message after signals contaminated by noise and different interferences. There are many different channel estimation methods, and block phase estimator [9] is used for simulations in this thesis. Details of this method can be found in the channel estimation model section.

Demodulation: In order to translate electric signals back to a binary sequence, a reverse process of mapping is needed to be done by the demodulator. Again, QPSK demodulation convert one signal level to 2 bits following this mapping:

$1 \rightarrow 00, j \rightarrow 01, -1 \rightarrow 11, -j \rightarrow 10.$ [8]

Burst Extractor: This part removes the guard bits and unique words that are added to the information bits. Next, the error between the information bits and the received bits is calculated.

2.3 Wireless Channel Model

In a wireless channel, signals radiate as electromagnetic waves through different objects. The physical environment attenuates the received power and therefore affects the bit error rate (BER) of the system. There are two types of fading in a wireless channel.

1. Long-term fading due to path loss and shadowing

Path loss is power dissipation by the transmitter and the channel through relatively large distance. Shadowing occurs when obstacles between the two ends attenuate the signal powers by absorption, reflection, scattering and diffraction [1]. Long-term fading is often leading to the fading effect on the channel with the log-normal probability distribution.

2. Short-term fading due to multipath and mobility.

Short-term fading varies received power over a relatively small distance and the signal wavelength is small as well. Different transmitted signals have different types of fading based on the signal characteristics such as bandwidth and channel parameters like delays. Generally there are two major types of fading; one is multipath delay spread, and the other one is Doppler spread.

For Multipath delay spread leads to time dispersion, which causes two different type of fading, called flat fading and frequency selective fading. In flat fading, the fluctuations of the channel gain caused by multipath change the strength of the signals over time, and multipath structure of the channel has the transmitted signals preserved in the receiver. Flat fading is the most common type of fading, and it affects the signal if

$$B_s \ll B_c \quad (2.1)$$

where B_s is the bandwidth of the signal and B_c is the bandwidth of the channel. Also the delay spread is less than the symbol period.

Frequency selective fading means the received signals have different types of transition waveforms that are attenuated and delayed in many different ways. Hence the received signals are distorted. It causes the channel to have inter symbol interference (ISI). Therefore the received signals are experiencing different levels of gains in different sections of the frequency spectrum. [2]

Other short term fading are fast fading and slow fading. They are classified based on the change of their symbol period and coherence time of the channel. They lead to frequency dispersion because of Doppler spreading, and then cause signal distortions. Fast fading has high Doppler spread when coherence time is less than symbol period. Slow fading has low Doppler spread when coherence time is greater than symbol period. [2]

In this thesis, it is assumed that the wireless channel is a Rician fading distribution channel. The most significant characteristic for Rician fading channel is that the nonfading (often Line of sight) component is dominating the propagation signals. Compared with this strong signal, other components with random multipath arrive with much weaker powers. If the dominate component fades away, the channel signal distribution will turn into a Rayleigh distribution.

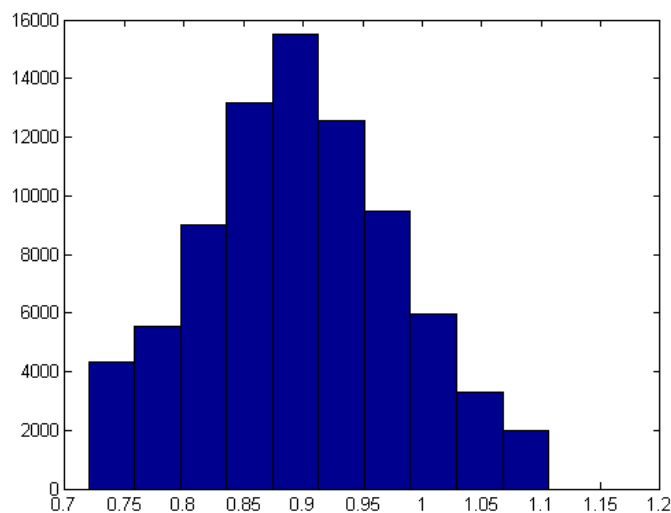


Figure 2-2 Rician Distribution Probability Distribution Histogram

The channel model used in this research is Jake's model [5], a simplified simulation of Clark's model [6]. This model has been used to simulate Rayleigh fading channel for a long time, and by adding the strong line of sight (LOS) component, it can be used to simulate Rician fading channel.

2.4 Multiple Input Multiple Output (MIMO) technology

The technology of MIMO uses more than one transmitting and receiving antennas to transfer more data in the communication system. This technology is used to increase data rates through multiplexing or to improve performance through diversity [1]. The two advantages of using MIMO is to increase the diversity of the system and to increase the number of transmitted symbols.

The main goal of diversity is to give the receiver side different replicas of the transmitted signals. For independent fading channels, the transmitted signals fade independently and the probability of having all the copies of the transmitted signals fading

simultaneously is very small. By selecting the signal with the highest SNR or by combining multiple signals, the receiver can decode the signals with higher reliability. The maximum diversity gain is equal to the product of the number of transmitting antennas and the number of receiving antennas. There are many ways to have independent fading paths in a wireless communication system, including space diversity, polarization diversity, frequency diversity, etc. In this thesis, the diversity gain is in the space-time domain and the independent channels are used without increase of transmitting power or bandwidth.

Besides increasing the diversity of the system, MIMO is also able to increase the transmitting data rate by increasing the number of transmitting and receiving antennas. With spatial multiplexing, the transmitted signals are split into two or more independent streams to be transmitted. The maximum multiplexing gain of the system is the minimum number of the number of transmitting antennas and receiving antennas. For example, in a system that has two transmit and receive antennas, the data rate can theoretically be twice as much as the original data rate with only one transmitting and receiving antenna. In each time slot, the system is transmitting two symbols at a time in a 2x2 (2 transmitters, 2 receivers) MIMO system.

However, there is a tradeoff between the diversity gain and multiplexing gain of the system. For a system that has N number of transmitting antennas and M number of receiving antennas, where spatial multiplexing gain r is an integer of $0, 1, \dots, \min(N, M)$, the maximum diversity gain $d(r) = (N - r)(M - r)$ as long as the block length is greater than $N + M - 1$. Figure 2-3 illustrates the tradeoff relationship between the spatial multiplexing gain and diversity gain. Figure 2-4 shows the communication system structure with space-time coding and decoding.

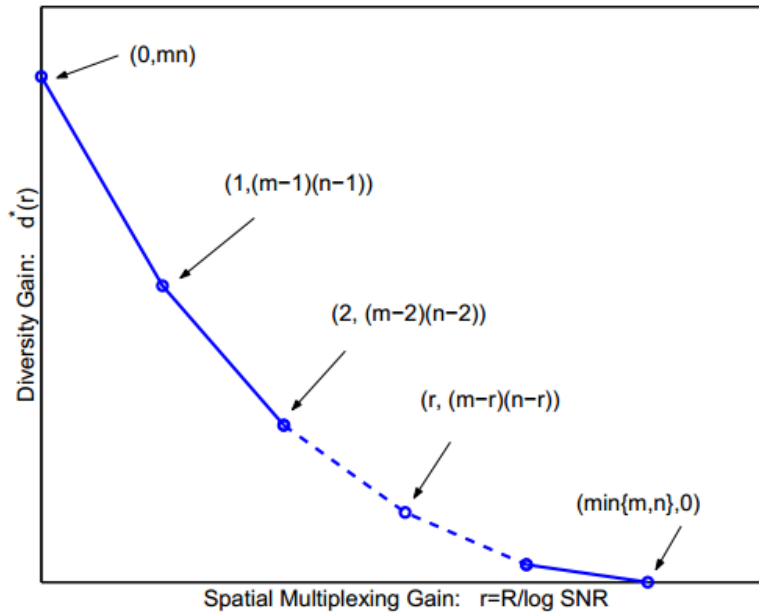


Figure 2-3 Optimal Tradeoff Between Spatial Multiplexing Gain And Diversity Gain

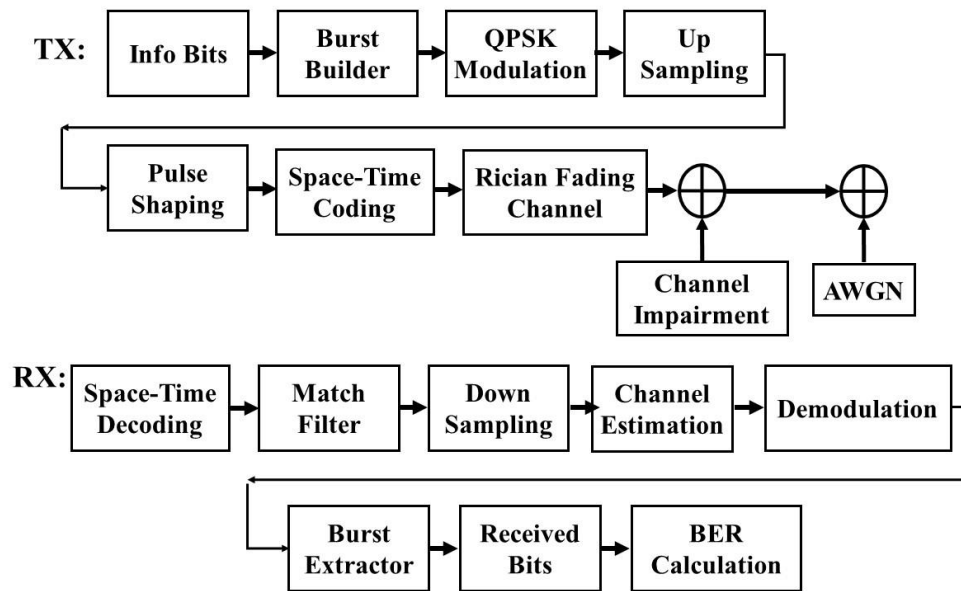


Figure 2-4 Space Time Coding Communication System Block Diagram

2.5 Alamouti Code

Low complexity system with space-time block code is used in order to reduce the complexity of decoding. In this thesis, Alamouti code is used as the space-time block coding. In a wireless communication system with two transmitting antennas and two receiving antennas, QPSK is used as the modulation scheme, which maps every 2 bits into one symbol and forming a constellation of 4 symbols, the transmitter first picks two symbols from the signals for the first time slot. At time one, s_1 is sent by antenna one and s_2 is sent by antenna two. At time two, $-s_2^*$ is sent by antenna one and s_1^* is sent by antenna two. Therefore, the codeword for transmitting is

$$S = \begin{bmatrix} s_1 & s_2 \\ -s_2^* & s_1^* \end{bmatrix} \quad (2.2)$$

During each time slot, one symbol is sent by one antenna and another symbol is sent by the other antenna.

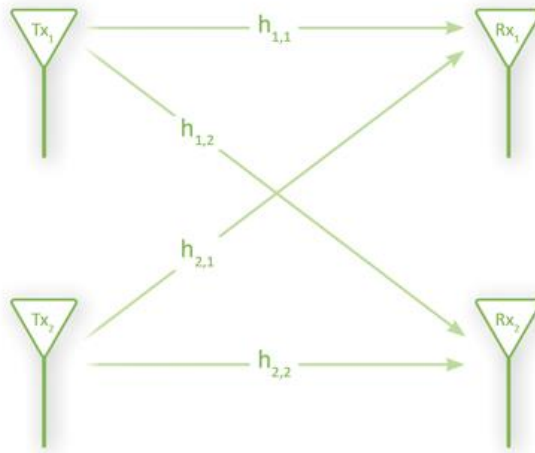


Figure 2-5 2x2 Alamouti Space-Time Block Code Antennas

In Figure 2-5, h_{ij} is the channel from the i th receiver to j th transmitter.

For a MIMO system, the received symbol y is

$$y = H.S + N \quad (2.3)$$

Where H is the channel matrix of Alamouti code, and N is the noise of the channel.

The received signals y in the first and second time slots are

$$\begin{bmatrix} y_1^1 \\ y_2^1 \end{bmatrix} = \begin{bmatrix} h_{11} & h_{21} \\ h_{12} & h_{22} \end{bmatrix} \begin{bmatrix} s_1 \\ s_2 \end{bmatrix} + \begin{bmatrix} n_1^1 \\ n_2^1 \end{bmatrix} \quad (2.4)$$

And

$$\begin{bmatrix} y_1^2 \\ y_2^2 \end{bmatrix} = \begin{bmatrix} h_{11} & h_{21} \\ h_{12} & h_{22} \end{bmatrix} \begin{bmatrix} -s_2^* \\ s_1^* \end{bmatrix} + \begin{bmatrix} n_1^2 \\ n_2^2 \end{bmatrix} \quad (2.5)$$

where s_1, s_2 are the transmitted symbols and n_n^t is the noise received by antenna n at time slot t . After combining both equations above, the equation becomes

$$\begin{bmatrix} y_1^1 \\ y_2^1 \\ y_1^{2*} \\ y_2^{2*} \end{bmatrix} = \begin{bmatrix} h_{11} & h_{21} \\ h_{12} & h_{22} \\ h_{21}^* & -h_{11}^* \\ h_{22}^* & -h_{12}^* \end{bmatrix} \begin{bmatrix} s_1 \\ s_2 \end{bmatrix} + \begin{bmatrix} n_1^1 \\ n_2^1 \\ n_1^2 \\ n_2^2 \end{bmatrix} \quad (2.6)$$

For the first receiver,

$$\begin{bmatrix} y_1^1 \\ y_1^{2*} \end{bmatrix} = \begin{bmatrix} h_{11} & h_{21} \\ h_{21}^* & -h_{11}^* \end{bmatrix} \begin{bmatrix} s_1 \\ s_2 \end{bmatrix} + \begin{bmatrix} n_1^1 \\ n_1^2 \end{bmatrix} \quad (2.7)$$

And for the second receiver,

$$\begin{bmatrix} y_2^1 \\ y_2^{2*} \end{bmatrix} = \begin{bmatrix} h_{12} & h_{22} \\ h_{22}^* & -h_{12}^* \end{bmatrix} \begin{bmatrix} s_1 \\ s_2 \end{bmatrix} + \begin{bmatrix} n_2^1 \\ n_2^2 \end{bmatrix} \quad (2.8)$$

Let $H_1 = \begin{bmatrix} h_{11} & h_{21} \\ h_{12}^* & h_{22}^* \end{bmatrix}$, and $H_2 = \begin{bmatrix} h_{11} & h_{21} \\ h_{12}^* & -h_{22}^* \end{bmatrix}$.

The Hermitian matrix, which is the conjugate and transpose of the original matrix H , is H^H . Therefore,

$$H_1 \cdot H_1^H = (\|h_{11}\|^2 + \|h_{21}\|^2) \cdot I \quad (2.9)$$

$$H_2 \cdot H_2^H = (\|h_{21}\|^2 + \|h_{22}\|^2) \cdot I \quad (2.10)$$

This is the orthogonal property of Hermitian Matrix. And by multiplying equation (2.3) by H^H , it becomes

$$H^H \cdot y = H \cdot H^H \cdot S + N \cdot H^H \quad (2.11)$$

Hence,

$$\begin{bmatrix} y_1^{1'} \\ y_1^{2'} \end{bmatrix} = H_1^H \cdot y = (\|h_{11}\|^2 + \|h_{21}\|^2) \begin{bmatrix} S_1 \\ S_2 \end{bmatrix} + \begin{bmatrix} n_1^{1'} \\ n_1^{2'} \end{bmatrix} \quad (2.12)$$

$$\begin{bmatrix} y_2^{1'} \\ y_2^{2'} \end{bmatrix} = H_2^H \cdot y = (\|h_{12}\|^2 + \|h_{22}\|^2) \begin{bmatrix} S_1 \\ S_2 \end{bmatrix} + \begin{bmatrix} n_2^{1'} \\ n_2^{2'} \end{bmatrix} \quad (2.13)$$

Therefore, by knowing the Channel H and receive symbols y, plus knowing the mean of $N \cdot H^H$ is zero, the transmitted symbols can be estimated by

$$\begin{bmatrix} S_1 \\ S_2 \end{bmatrix}^{\sim} = (H \cdot H^H)^{-1} H^H \begin{bmatrix} y_1^1 \\ y_2^1 \\ y_1^{2*} \\ y_2^{2*} \end{bmatrix} \quad (2.14)$$

By using the minimum distance decision, the estimated transmitted symbols is estimated by combining the received signals, and finding the one with the minimum absolute value.

$$S_1^{\sim} = \underset{S_i}{\operatorname{argmin}} \sum_{i=1}^M \|y_i^1 - (\|h_{1i}\|^2 + \|h_{2i}\|^2) \cdot S_i\| \quad (2.15)$$

$$S_2^{\sim} = \underset{S_i}{\operatorname{argmin}} \sum_{i=1}^M \|y_i^2 - (\|h_{1i}\|^2 + \|h_{2i}\|^2) \cdot S_i\| \quad (2.16)$$

In equations (2.15) and (2.16), S_i is all the possible symbols in the modulation scheme. M is the number of receive antennas. In this thesis, M=2. The 2x2 MIMO system is using the above encoding and decoding scheme.

2.6 Channel Estimation Model

In the constellation diagrams below, the symbols are all scattered after signals pass through Rician fading Channel with AWGN noise.

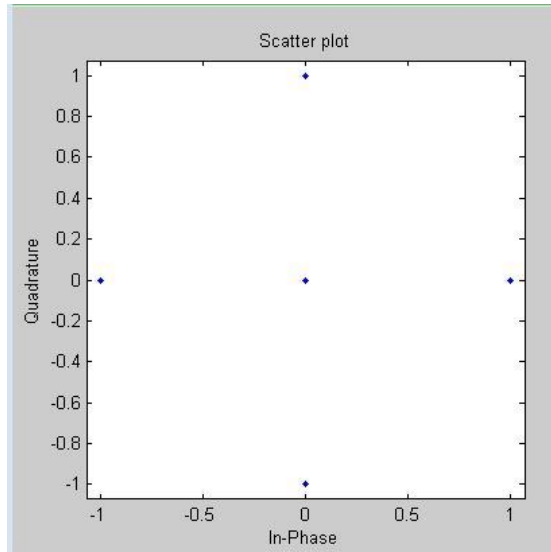


Figure 2-6 QPSK Modulation Symbols

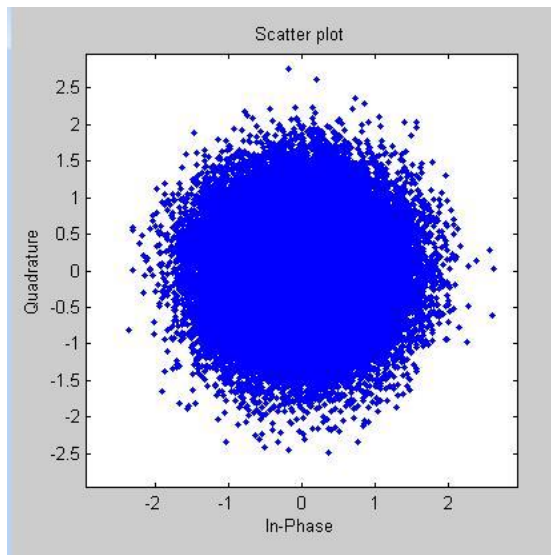


Figure 2-7 Symbols with AWGN noise

See Figure 2-6 and Figure 2-7 for illustration of symbols before and after the channel and noise. In this thesis block phase estimation algorithm by Viterbi [9] is used as the channel estimation method. The channel estimation method is only used in the single input single output (SISO) system.

Here are general steps of the channel estimation:

Step 1: Raise the received signal amplitudes by 2 and its phase values by 4. Define a sliding window of 10 symbols and use unique words to remove phase ambiguity. According to Viterbi's paper [9], the received signal is

$$r(n) = p \cdot e^{j\phi(n)} \quad (2.17)$$

where p is the absolute value of the signal. After raising the power to 4, it becomes

$$(r(n))^4 = p^2 \cdot e^{j4\phi(n)} \quad (2.18)$$

With the window size defined to be 10 symbols, a sample with size N symbols is collecting all the signal phase values from the first symbol to the N symbol in the sequence. In this simulation, $N=71$. The bigger N is, the more accurate the estimated phase, but it also takes more computation power. For the first sample set, let

$$\varphi = \tan^{-1} \left\{ \frac{\text{real} \left[\frac{1}{N} \sum_{n=1}^N p^2 \cdot e^{j4\phi(n)} \right]}{\text{img} \left[\frac{1}{N} \sum_{n=1}^N p^2 \cdot e^{j4\phi(n)} \right]} \right\} + k\pi \quad (2.19)$$

For all phases,

$$\theta \left(\frac{N-1}{2} \right) = \frac{\varphi}{4} + \frac{k\pi}{4} \quad (2.20)$$

Therefore, the first estimated phase is $\theta(35)$. Then $\theta(45)$ can be obtained the same way by sliding the window to get all the phase values of the next sample set. With this approach, $\theta(45), \theta(55) \dots$ can be calculated, until the number of collected symbols are less than the size of sample set.

Step 2: A reference phase is needed in order to compare the difference between the received symbols and the original symbols. Since the unique word sequence and its location in the burst structure is known, the symbols in the same location of the received data are compare with each other. There are 48 unique word symbols in this simulation, therefore

$$\theta(ref) = \frac{1}{48} \sum_{i=1}^{48} phase \left(\frac{r(i)}{uw(i)} \right) \quad (2.21)$$

the $r(i)$ is a received symbol and 48 symbols are taken in the same position of the unique word. In the equation above, $uw(i)$ is an original unique word. $\theta(ref)$ is an reference phase and a key value to estimate the actual phases of the received symbol. And let's define a parameter to determine the value of k for the estimated phase,

$$\hat{k} = \min \left| \theta(ref) - \left(\frac{\varphi}{4} + \frac{k\pi}{4} \right) \right| \quad (2.22)$$

where k has the value of either $\pm 1, \pm 2, \pm 3, \pm 4$ or 0. \hat{k} is the minimum value of k when $\left(\frac{\varphi}{4} + \frac{k\pi}{4} \right)$ and $\theta(ref)$ have the closet value. By inserting \hat{k} ,

$$\theta(35) = \frac{\varphi}{4} + \frac{\hat{k}\pi}{4} \quad (2.23)$$

where $\theta(35)$ is the first estimated phase.

Step 3: Slide the window by 10 symbols, and collect values of the next 71 symbols to compute φ . Using $\theta(35)$ as the next reference phase to calculate \hat{k} for the estimation of $\theta(45)$. By repeating this method, every $(35+10 \cdot x)$ symbol phases can be estimated, where x is a positive integer.

For other symbols in between, we use interpolation to get the symbol phase.

Step 4: Perform channel compensation by letting

$$r'(n) = r(n) \cdot e^{-j\theta(n)}$$

where $\theta(n)$ is the estimated phase above. Then the phases of $r'(n)$ can be estimated by the hard slicer below

$$\text{if } \begin{cases} -\frac{\pi}{4} < phase < \frac{\pi}{4}, & \text{symbol is 1} \\ \frac{\pi}{4} < phase < \frac{3\pi}{4}, & \text{symbol is i} \\ -\frac{\pi}{4} > phase > -\frac{3\pi}{4}, & \text{symbol is -i} \\ \text{else,} & \text{symbol is -1} \end{cases}$$

After all 4 steps, received symbols are now ready to map it back to bits.

Chapter 3

Radio Frequency (RF) Channel Impairments

3.1 Introduction

In modern wireless communication systems, direct conversion receiver (DCR) is incorporated with many applications including television and cell phones. It uses synchronous detection to demodulate signals coming in. A local oscillator produces a frequency that is very close to the incoming one. This receiver simplifies the circuit design and therefore was widely used in the IEEE 802.11a/g wireless LAN standards. Particularly for orthogonal frequency division multiplexing (OFDM) scheme, DCR is used to improve efficiency. Although it has many advantages on filtering unwanted signals with low cost and power consumption, it also creates a direct current offset (dc offset) and IQ imbalance to the system. [10]-[13]

The local oscillator signal is responsible for the dc offset, because it mixes itself to zero intermediate frequency. Furthermore, the dc offset is also generated by the effect of analog offset in the baseband circuit in the transmitter. Many RF components also contribute to the dc offset including effects of transistor mismatch and amplifier intermodulation. The digital-to-analog converter in the transmitter side and the analog to digital converter in the receiver side play a big part in the generation of dc offset. [14]

IQ imbalance was the imbalance of the components in the in-phase (I) and quadrature (Q) phase. In a normal scenario, the angle between I and Q is supposed to be 90 degrees. However, phase mismatch affects the I and Q angle and hence it is no longer 90 degrees. These effects create distortions in the signals and later affects the accuracy of the received signal.

Phase noise is a random variation of the phase in the IQ plane. Complex signals with phase noise have its phases added by random values and scatter in random

directions. In many wireless communication systems, such as OFDM over a fading channel, phase noise is caused by the instability of the oscillator. An oscillator generates phase noise on the modulation carriers, and the RF sine waves. In contrast to the IQ imbalance phase shift, the angle of the phase shifted by noise is random. [17]

All the DC offset, IQ imbalance and phase noise effect on the wireless systems need to be evaluated in order for telecommunication engineers to decide what kind of compensation scheme they want to use to deal with channel impairments. This depends on the channel characteristics and the signal to noise ratio. In some cases two or all three effects can affect the system at the same time. Therefore different scenarios of simulation have been set up to present the system performance under various cases.

3.2 DC Offset Model

In this thesis, the effect of dc offset on Rician fading channel is evaluated. For the issue of DC offset, there are some compensation schemes that can be used to eliminate the DC offset from the wireless channel including maximum likelihood criterion [16], differential filters [15], and high pass filters [15]. Without compensations, the distortions of the signals result into the degradation of dB gains in the BER performance. These simulations can help RF engineers to decide whether the effects are large enough to use compensation schemes, when signals are crossing Rician fading channel.

The DC offset is added to the system by inserting a DC offset signal to the received signal after it passed through the fading channel and before AWGN noise is added to the signal. In the MIMO system, the DC offset signals are added to both received signals independently. The DC offset signal always starts with an element with value of zero, and increase each element value continuously, until it reach the last element with the value that is five percent of the maximum received signal value. For every simulation trial, the

maximum value of the signal can be different since the bits are randomly generated and the channel fades following the Rician probability distribution.

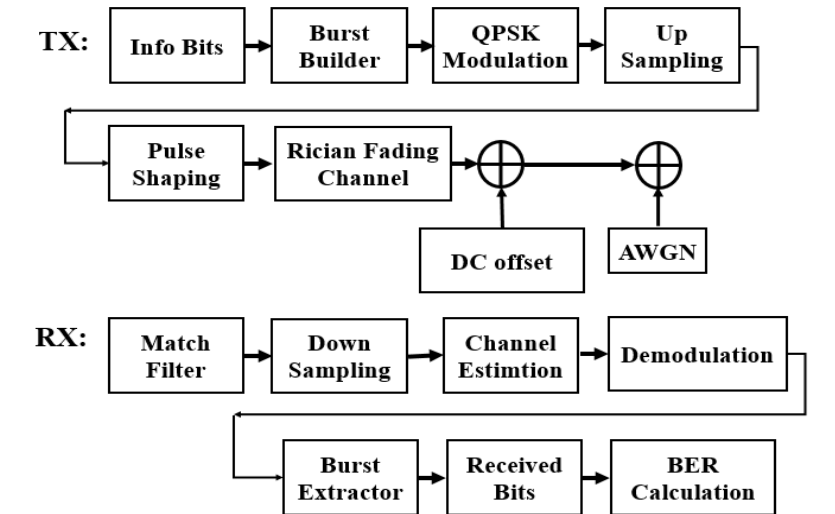


Figure 3-1 DC Offset Interference Block Diagram

Figure 3-1 illustrates where the DC offset is added to the wireless system. This simulation focuses mainly on the system and signal level design. It has no attention given to the circuit level design of the DC offset.

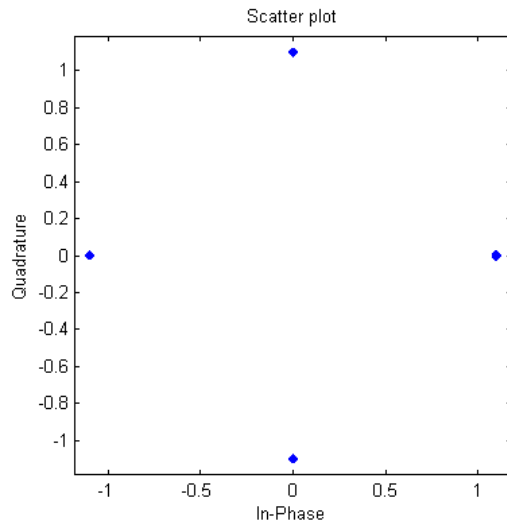


Figure 3-2 Modulated Symbol

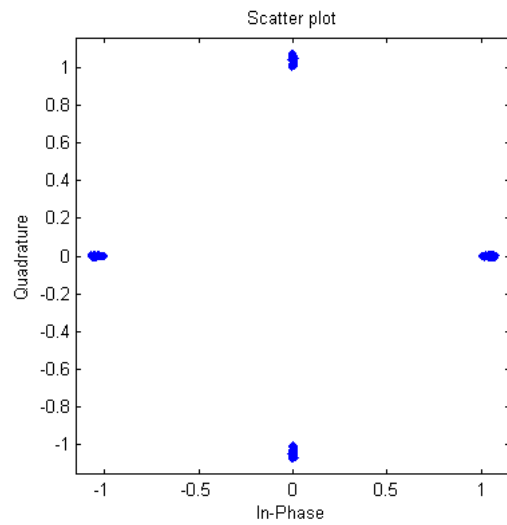


Figure 3-3 Symbols with DC Offset Interference

Figure 3-2 and 3-3 are constellation diagrams of the modulated symbols before and after DC offset impacts the system. Compare to the symbols before, the DC offset symbols all increases in magnitude and spread out, and causes DC imbalance.

3.3 DC Offset Simulation Results

In the Figure 3-4, Figure 3-5 and Figure 3-6 below, the bit error rate (BER) performances of the Rician fading channel are calculated by simulations of the models discussed above. The x axis of the figure shows the SNR ratio of the system, with the increment of 1 dB. The y axis of each figure is the BER of the system. The BER performances of the raw single input single output (SISO) and MIMO wireless system are also plotted in the figures. In all dB loss measurements of this thesis, the BER values at 2% BER are used for calculations.

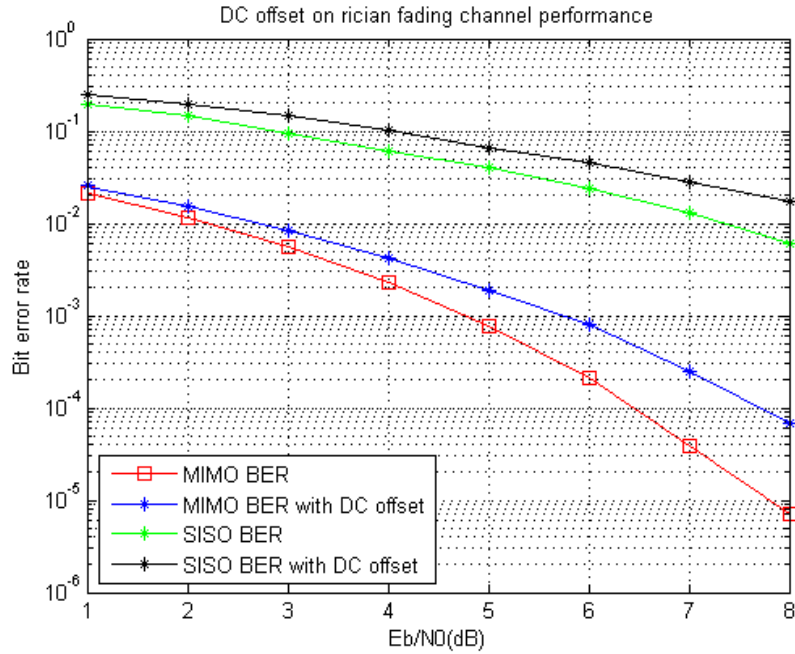


Figure 3-4 DC Offset BER Performance for $k = 7$ dB, $f_d = 20$ Hz

Figure 3-4 shows the system with DC offset BER performance of the Rician fading channel with $k = 7$ dB and $f_d = 20$ Hz. The dB loss caused by DC offset in the SISO system is 1.4 dB. The dB loss caused by dc offset in MIMO system is 0.2 dB. The DC offset has a more significant impact to the SISO system.

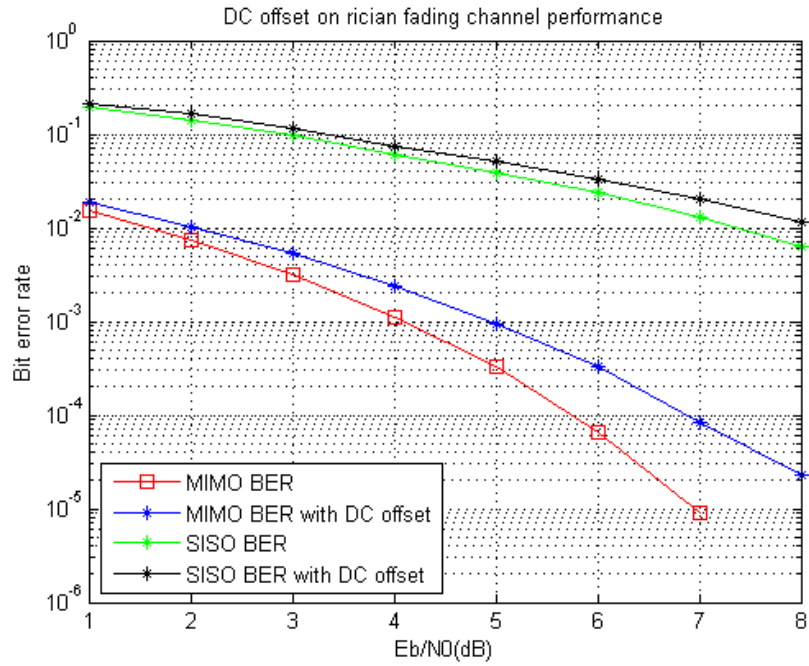


Figure 3-5 DC Offset BER Performance for $k = 12\text{dB}$, $f_d = 100\text{Hz}$

Figure 3-5 shows the system with DC offset BER performance of the Rician fading channel where $k = 12\text{ dB}$, $f_d = 100\text{ Hz}$. The dB loss caused by DC offset in the SISO system is 0.7 dB. The dB loss caused by DC offset in MIMO system is 0.15 dB. The DC offset has more significant impact to the SISO system and does not impact the MIMO system much.

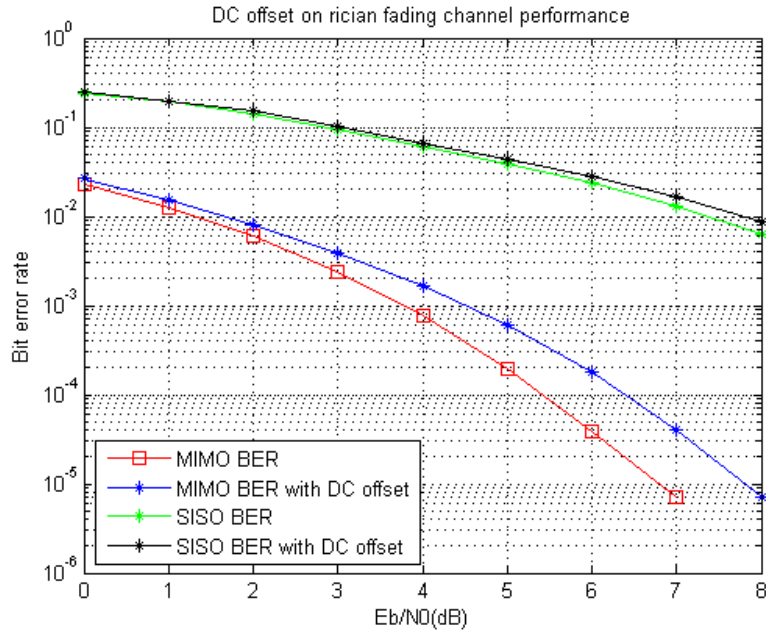


Figure 3-6 DC Offset BER Performance for $k = 200$ dB, $f_d = 0$ Hz

Figure 3-6 shows the system with DC offset BER performance of the Rician fading channel where $k = 200$ dB and $f_d = 0$ Hz. The dB loss caused by DC offset in the SISO system is 0.2 dB. The dB loss caused by DC offset in a MIMO system is 0.1 dB. The DC offset does not impact much to either the SISO or MIMO system. These systems have weak scatter path components and no Doppler shift.

From Figure 3-4 to Figure 3-6, it is obvious that as the SNR ratio increases, which in these cases mean the AWGN noise is decreasing, the BER of the system decreases, which means the performances of the system are getting better when there is less noise. The curves of the plots with DC offset are similar to the plots without DC offset. Through these simulations, it is concluded that the MIMO system is more reliable than SISO system when a system is experiencing DC offset.

3.4 IQ Imbalance model

In order to find solutions for the IQ imbalance variation in wireless system, many calculation methods were proposed. One of these is the IQ imbalance estimation scheme by Mamiko [15]. With the occurrence of IQ imbalance in wireless system, the evaluation of the IQ imbalance with Rician fading channel is necessary. These simulation results will give people a better idea of how IQ imbalance impacts the accuracy of received wireless data. It will also help them to decide whether it is worth to come up with a compensation scheme to cancel the effect.

In this thesis, the phase shift of the complex signals is conducted after the signals pass through the Rician fading channel. After all signals experience fading in the wireless channel, their IQ phases are already out of its original phase by a certain degree. Based on their current phase, a constant shift of 5 degrees is applied to each of the signal phase, which means the phase of all the signals are shifted in the same direction.

The IQ imbalance is performed after the signals fade with the Rician distribution and before the noise of AWGN is added. Figure 3-7 shows a system block diagram of the IQ imbalance model. In MIMO system, the IQ imbalance is applied to each individual receiver.

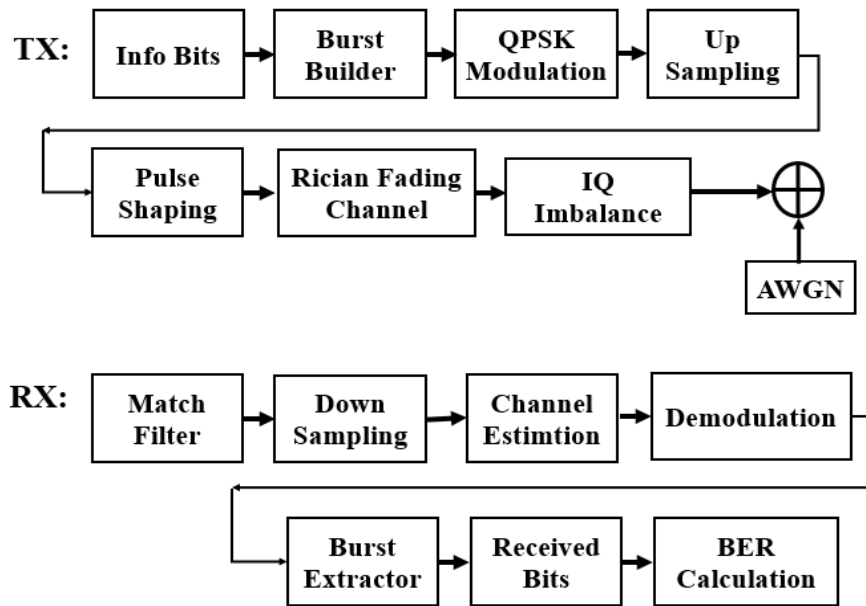


Figure 3-7 IQ Imbalance Interference Block Diagram

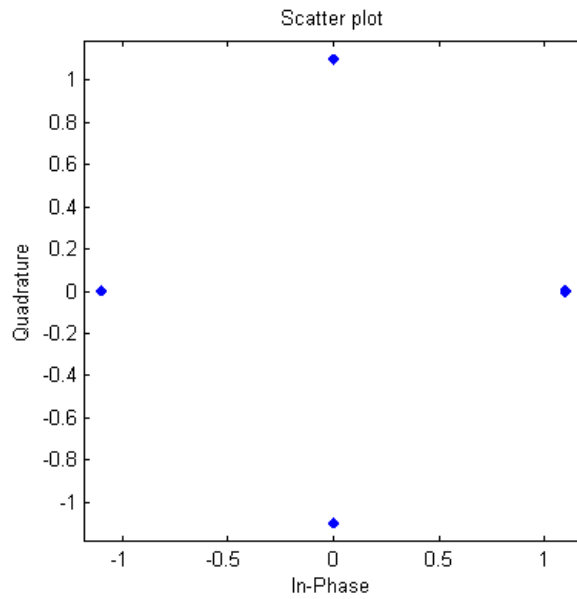


Figure 3-8 Modulated Symbols

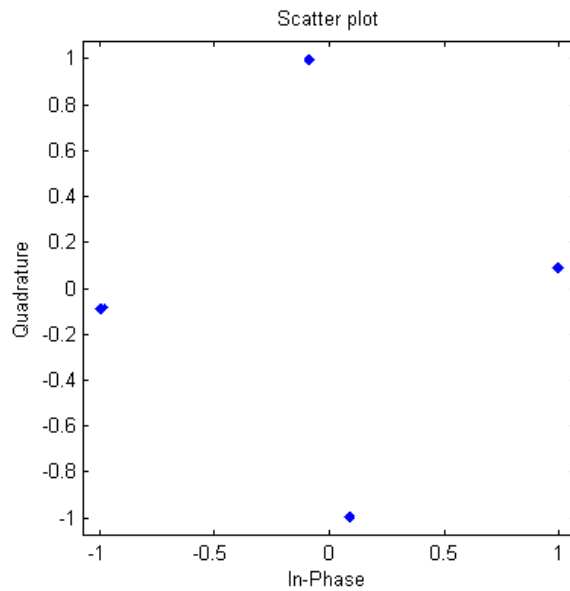


Figure 3-9 Symbols with IQ Imbalance

Figure 3-8 shows the constellation diagram of the complex signals after it passes through the Rician fading channel. Figure 3-9 shows the constellation diagram after IQ imbalance was applied. There is a phase shift of the symbols and they all shift to one direction.

3.5 IQ Imbalance Simulation Results

The IQ imbalance adds to the system after the complex signals pass through the Rician fading channel. The angles of the complex signals are calculated first. Then adds 5 degree of phase shift to each of the phase value. Many IQ imbalance estimation methods have indicated that the phase shifts are normally set to 5 degrees [15] for IQ imbalance, therefore 5 degrees shift to one direction is set as the phase shift magnitude in these cases. Similar to the simulations of DC offset, the BER performance is calculated one thousand times with each SNR value, with an increment of 1 dB. Then the average BER value is

found for each SNR. The simulated IQ imbalance BER is used to compare with the raw BER without IQ imbalance in order to find out the dB loss due to the IQ imbalance of 5 degrees in both the SISO and MIMO system.

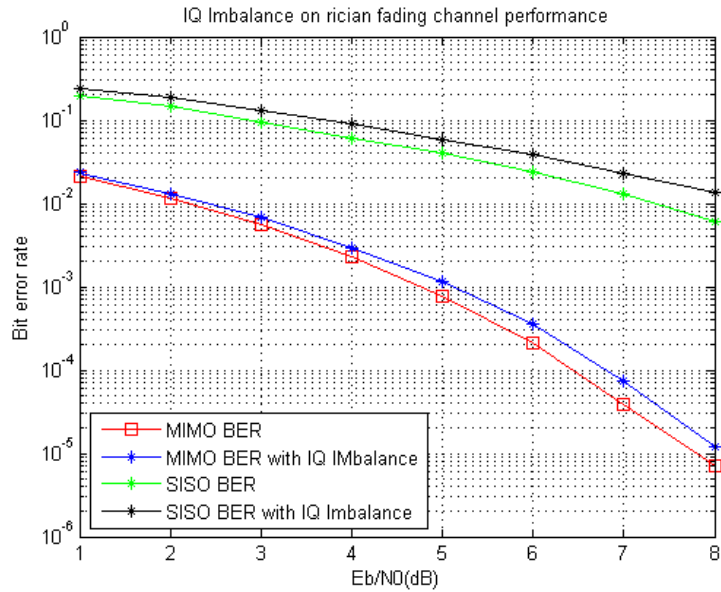


Figure 3-10 IQ Imbalance BER Performance for $k = 7$ dB, $f_d = 20$ Hz

Figure 3-10 shows the system with IQ imbalance BER performance of the Rician fading channel where $k = 7$ dB, $f_d = 20$ Hz. The dB loss caused by IQ imbalance in SISO system is 0.9 dB. The dB loss caused by IQ imbalance in MIMO system is 0.05 dB. The IQ imbalance has a more significant impact to the SISO system.

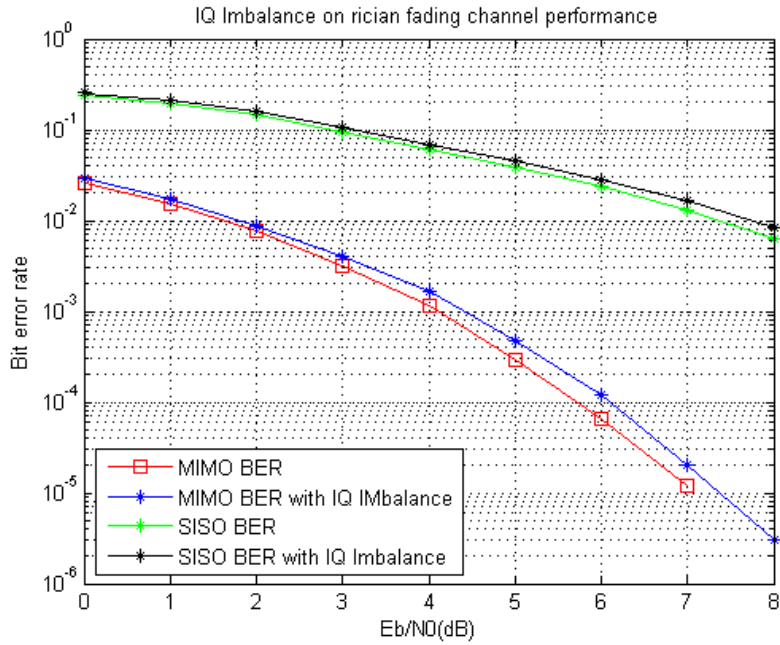


Figure 3-11 IQ Imbalance BER Performance for $k = 12$ dB, $f_d = 100$ Hz

Figure 3-11 shows the system with IQ imbalance BER performance of the Rician fading channel where $k = 12$ dB, $f_d = 100$ Hz. The dB loss caused by IQ imbalance in SISO system is 0.15 dB. The dB loss caused by IQ imbalance in MIMO system is 0.05 dB. As the scatter path components get weaker and Doppler shift increases, the MIMO system is still more reliable than SISO system.

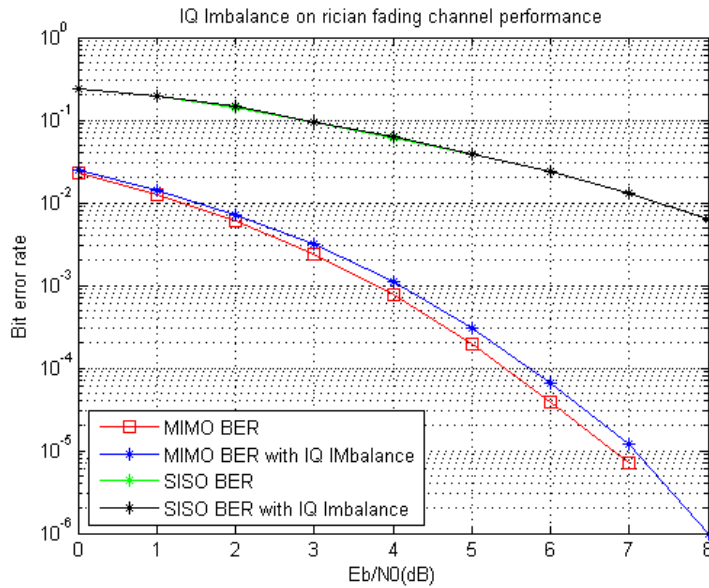


Figure 3-12 IQ Imbalance BER Performance for $k = 200$ dB, $f_d = 0$ Hz

Figure 3-12 shows the system with IQ imbalance BER performance of the Rician fading channel where $k = 200$ dB, $f_d = 0$ Hz. The dB loss caused by IQ imbalance in SISO system is 0 dB. The dB loss cause by dc offset in MIMO system is 0.05 dB. This time under no Doppler shift scenario, IQ imbalance has no impact to SISO. However, there is some dB loss for the MIMO system.

From the system with IQ imbalance BER performance above, there is not much dB loss until the AWGN noise gets small in the system. This indicates that under this system model the 5 degree IQ imbalance has very little impact to the system performance, for both a SISO and a MIMO system.

3.6 Phase Noise Model

Similar to the IQ imbalance case, many estimation schemes have been proposed to find out the effects of phase noise in the wireless communication channel. Most of the

work done with an OFDM signals, such as [18][19]. In this thesis, the investigation of the phase noise influence to Rician fading channel system is conducted.

In the simulation, phase noise is added to the complex signals after going through the Rician fading channel. For MIMO, phase noise is added to each received signals. Figure 3-13 is a block diagram to illustrate where phase noise is added to the system.

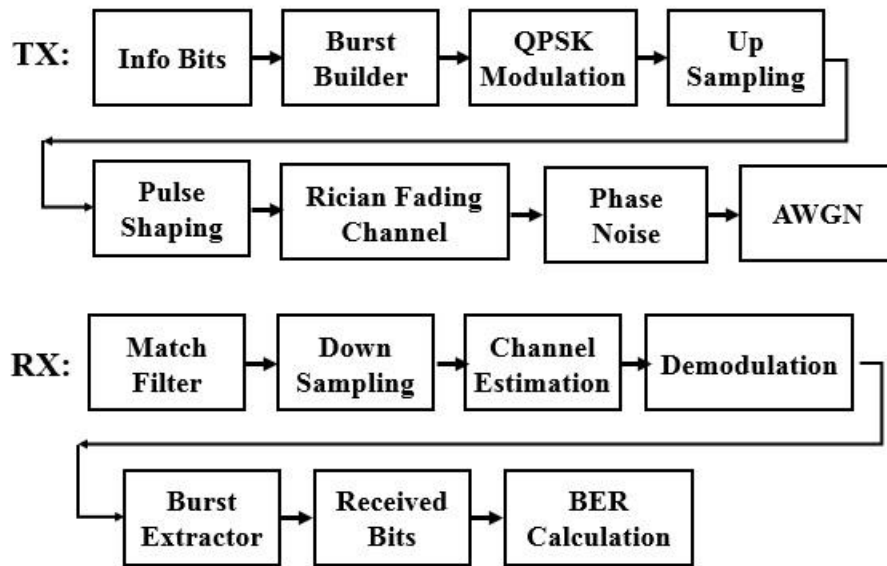


Figure 3-13 Phase Noise Interference System Diagram

In this case, the phases of the complex signals are calculated after passing through the Rician fading channel. When adding phase noise to the system, even though the phase shift is random, a limit of 10 degrees shift is set according to the practical environment.

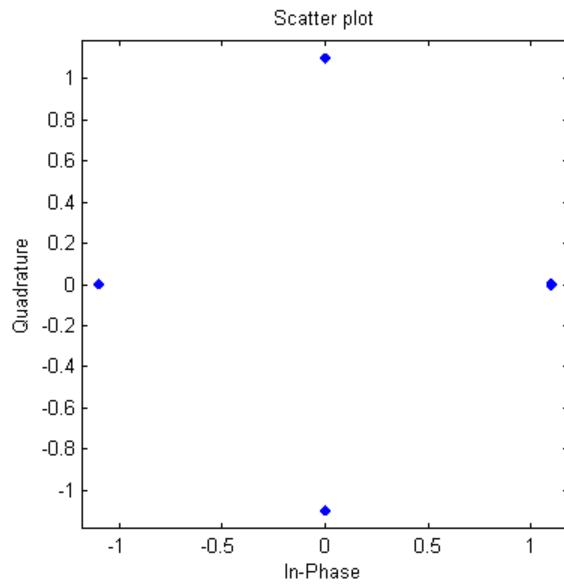


Figure 3-14 Modulated Symbols

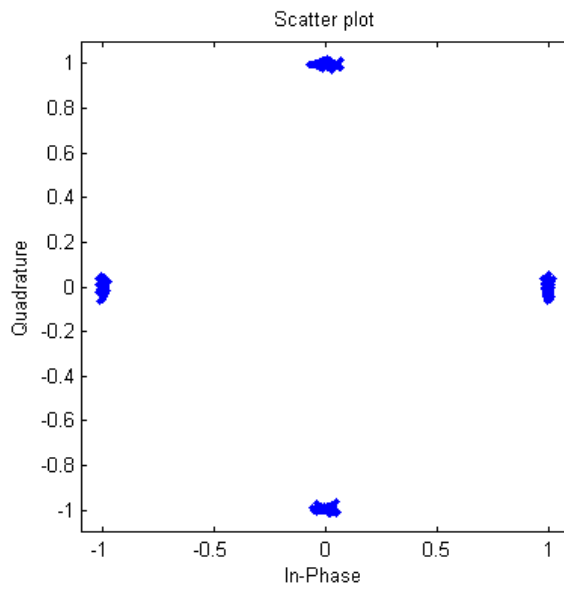


Figure 3-15 Symbols with Phase Noise

Figure 3-14 shows the constellation diagram of the complex signal after it passes through the Rician fading channel. Figure 3-15 shows the constellation diagram after phase noise is applied to the system. There is a scattering effect to the symbols in the constellation diagram after adding phase noise. The phases of the symbols are shifted in all different directions. This is different from the IQ imbalance constellation diagram, which all the symbols have phase shifts in one direction.

3.7 Phase Noise Simulation Results

The simulation adds phase noise to the modulated signals after passing through the Rician fading channel. The angles of the complex symbols are calculated and a plus or minus phase shift is added to each angle, randomly from 0 degrees to 10 degrees. In reality, there is no way to predict the exact value of the phase noise, so an estimation of range is used. Similar to the simulation of IQ imbalance, the average BER performance is obtained by running the simulation one thousand times with each SNR value, with an increment of 1 dB. At each increment the average BER value for each SNR is found. The simulated system BER with phase noise is compared with the system BER without phase noise in order to find out the dB loss due to phase noise.

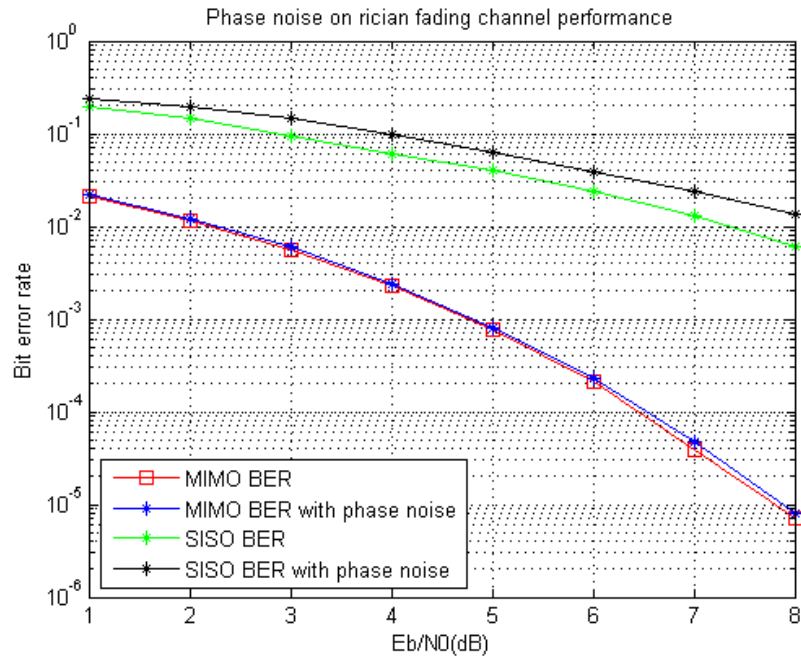


Figure 3-16 Phase Noise BER Performance for $k = 7$ dB, $f_d = 20$ Hz

Figure 3-16 shows the system with phase noise BER performance of the Rician fading channel where $k = 7$ dB, $f_d = 20$ Hz. The dB loss caused by phase noise in SISO system is 1 dB. The dB loss caused by phase noise in MIMO system is 0 dB. The phase noise has some influences to the SISO system but not to the MIMO system at all.

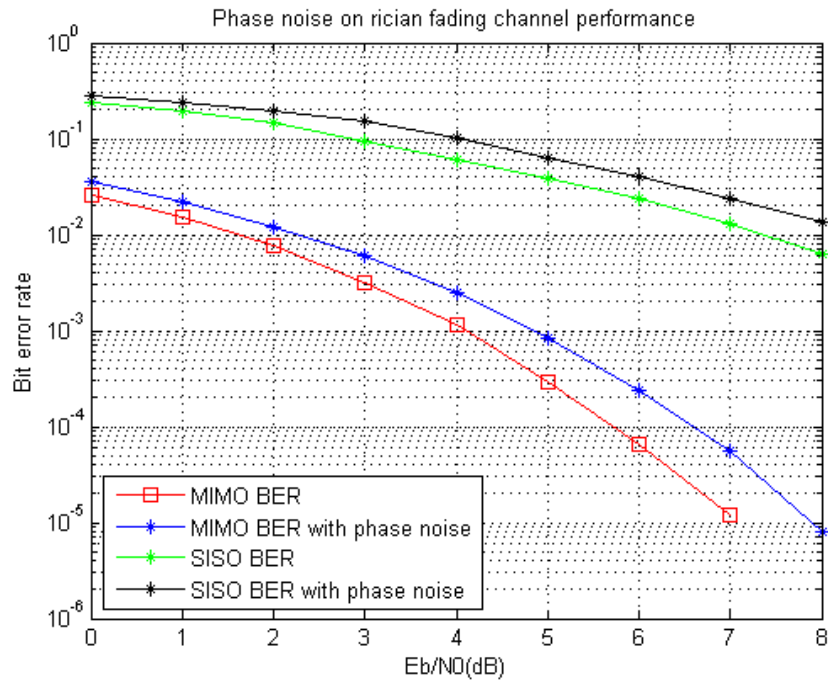


Figure 3-17 Phase Noise BER Performance for $k = 12\text{dB}$, $f_d = 20\text{Hz}$

Figure 3-17 shows the phase noise on Rician fading channel BER performance where $k=12\text{dB}$, $f_d=100\text{Hz}$. The dB loss caused by phase noise in the SISO system is 1 dB. The dB loss caused by phase noise in the MIMO system is 0.5 dB. The phase noise has some impact on both systems, but MIMO is more reliable comparing to SISO in the scenario of small Doppler shift and weak scatter path components.

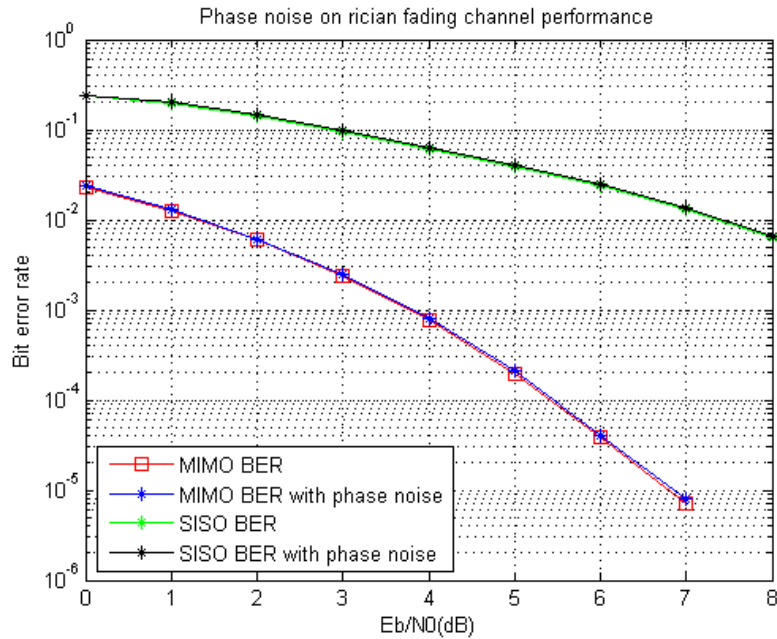


Figure 3-18 Phase noise BER Performance for $k = 200$ dB, $f_d = 0$ Hz

Figure 3-18 shows the phase noise on Rician fading channel BER performance where $k = 200$ dB, $f_d = 0$ Hz. The dB loss caused by phase noise to both systems are 0 dB. When scatter path components are weak and the channel has no Doppler shift, the phase noise does not impact both the MIMO and the SISO system.

From the system with phase noise BER performance in different scenarios, dB losses are not quite the same. With large Doppler shifting, the dB losses are generally more significant to both systems. The curves of the plots are similar for both the original system plots and the system with phase noise. While experiencing phase noise impact, MIMO systems have less dB losses than SISO systems, even though the differences are small.

Chapter 4

Co-Channel Interferences

4.1 Introduction

In modern wireless communications, the channel that is used by one transmitter to communicate with its receiver sometimes overlaps with other channels that are used by the other transmitters and receivers. For the cellular networks today in the telecommunication industry, frequency spectrum is very precious and spectrum space is expensive to buy. In ideal cases, the frequency spectrum should be divided into different frequencies and assigned to different cells. However, in certain geographic locations, the frequency are re-used. For a single cell, channel around the cell can all be using the same frequency [20]. The two channels can share the exact same frequency spectrum, which causes co-channel interference (CCI), or having part of the frequency spectrum interfere with each other, which leads to adjacent channel interference (ACI) [4].

Other factors such as poor network planning and rare high pressure weather conditions also contributed to the effect of co-channel interference. In mobile communications, a radio link performance is often limited by CCI rather than noise [21]. In this thesis, the impact of CCI to Rician fading channel of a wireless system is evaluated.

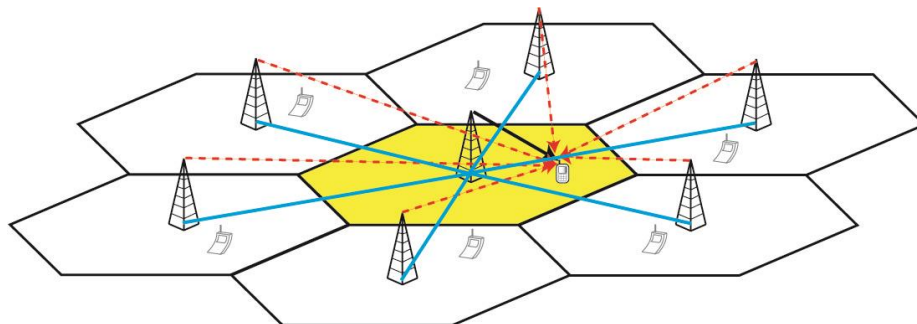


Figure 4-1 Co-Channel Interference in MIMO System

Figure 4-1 is an example of *multiple-input and multiple-output* (MIMO) multicarrier network. It illustrates how CCI arises in the long time evolution (LTE) advanced network. CCI is caused by its simultaneous transmissions on the same frequency from all the surrounding base stations of the central base station [22]. It reduces the data rates of the system and impacts the accuracy of the received data, especially for users at the cell edge.

4.2 Co-Channel Interference System Model

There are two ways to eliminate or reduce the effect of CCI in a wireless communication system. One is to restructure the architecture of the wireless network such as control level cooperation and full level cooperation. The other one is to have compensation scheme to cancel the effect of CCI [22]. The ratio between the received signals and the interference signals is called the signal to interference ratio (SIR). In the simulation, the CCI impact on the Rician channel wireless system performance is evaluated.

All the simulations in this section are run with different SIR value to get a clear evaluation of the effect of CCI. The assumption made in the simulations is that the interference channel is the also a Rician fading channel. There is only one channel that is interfering with the system channel in this wireless system model.

The CCI interference will be added to the complex signals after signals transmitted through the Rician fading channel. The CCI signals is generated by another wireless system that has the same QPSK modulation and fading channel. In the simulation, only part of the signals are added to the current system, depending on the SIR. IN MIMO system, CCI is also added to the receiver before adding AWGN noise. In this thesis, the SIR ratios are 5dB, 10dB, 15dB and 20dB. Figure 4-2 is a block diagram that illustrates where CCI adds to the wireless system.

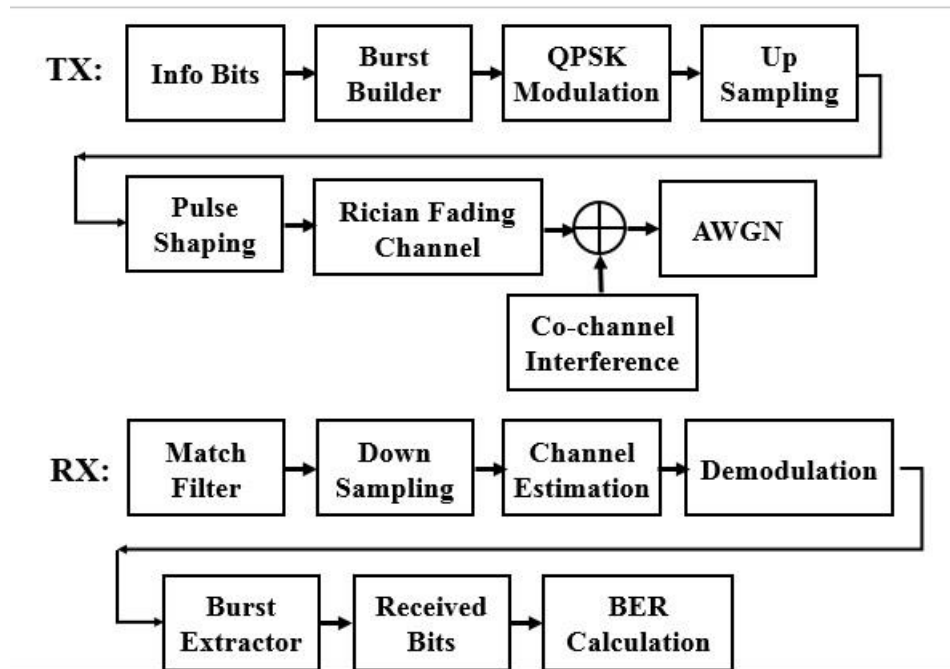


Figure 4-2 Co-Channel Interference System Block Diagram

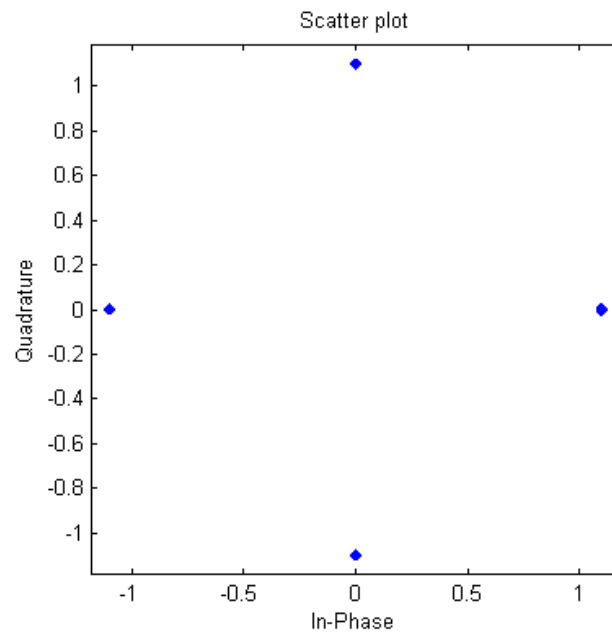


Figure 4-3 Modulated Symbols

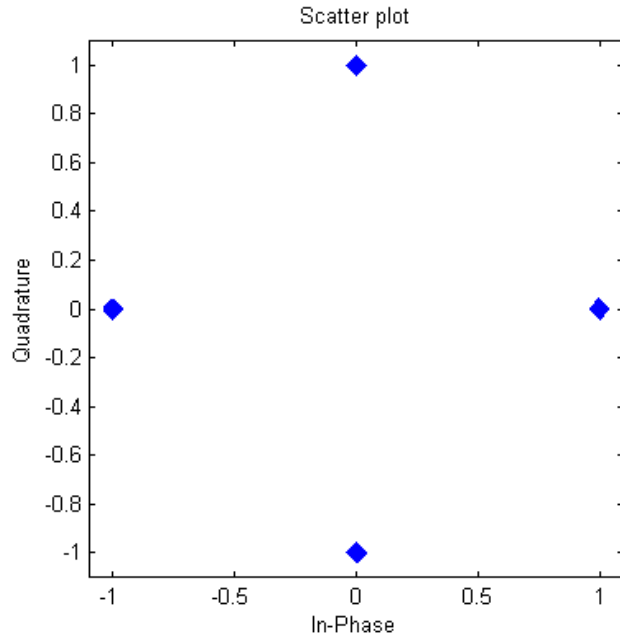


Figure 4-4 Symbols with Co-Channel Interference

Figure 4-3 shows the constellation diagram of the complex signals after passing through the Rician fading channel. Figure 4-4 shows the constellation diagram of the symbols after CCI is applied to the system. Base on Jiang Li and Qilian Liang's work [21], the symbols after fading are defined as $r'(k)$, the CCI is $u(k)$ and the AWGN noise $e(k)$, therefore the received signal $r(k)$ before going into the channel estimator is

$$r(k) = r'(k) + u(k) + e(k) \quad (4.1)$$

The CCI $u(k)$ is expressed as

$$u(k) = \sum_{j=1}^N u_j(k) = \sum_{j=1}^N \sum_{i=0}^{n_j} b_{ij}(k) s'_j(k-i) \quad (4.2)$$

In the equation 4.2, $s'(k)$ is the QPSK transmitted symbol and n_j is the j th co-channel order, in this case $n_j = 1$ since there is only have one co-channel. $b_{ij}(k)$ is the corresponding channel gain where $i = 0, 1, 2, 3 \dots$

4.3 Co-Channel Interference Simulation Results

The simulation adds the co-channel interference to the modulated signals after passing through the Rician fading channel. The signal to noise (SIR) ratios are set to 5 dB, 10 dB, 15 dB and 20 dB. The average BER performance is obtained by running the simulation one thousand times with each SNR value, with increment of 2 dB. The system performance with Co-channel interference (CCI) is used to compare with the system without CCI BER in order to find out the dB loss due to CCI.

Only plots with 5 dB SIR and 20 dB SIR are shown in this thesis, dB losses for 10dB and 15dB SIR are recorded in the tables of Chapter 6.

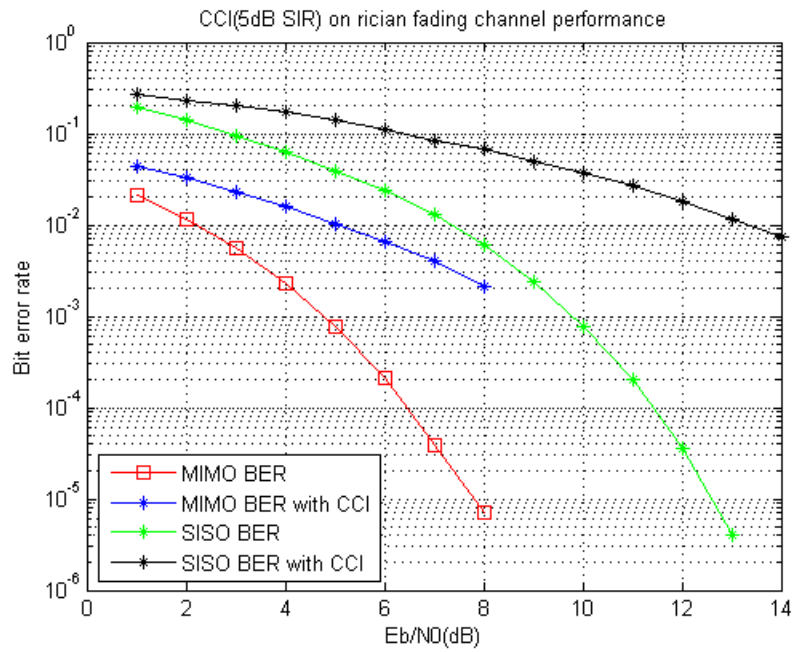
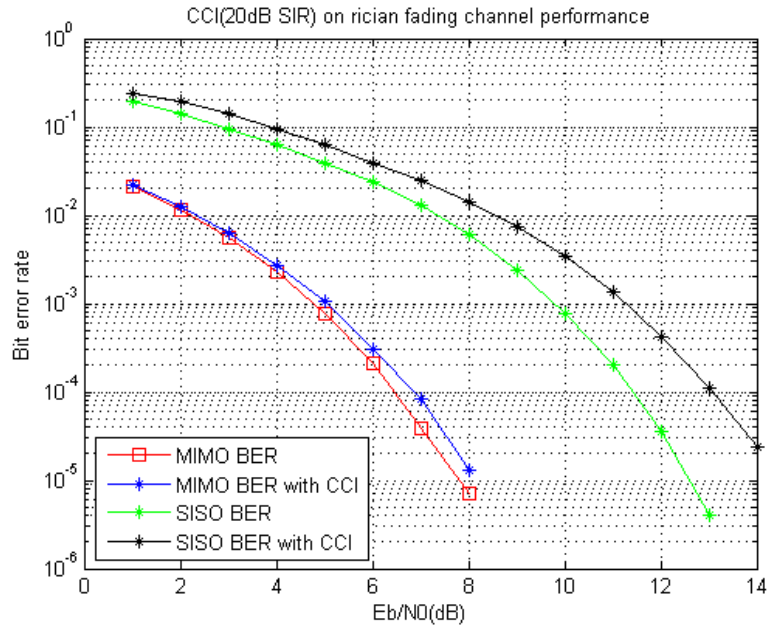


Figure 4-5 CCI BER Performance for $k = 7$ dB, $f_d = 20$ Hz

Figure 4-5 shows the Rician fading channel system with CCI BER performance where $k = 7$ dB, $f_d = 20$ Hz, with different SIR value. For 20 dB SIR, the dB loss caused by CCI in SISO system is 1 dB. The dB loss caused by CCI in MIMO system is 0dB. The CCI has some influence to the SISO systems but not to the MIMO system at all.

For 5 dB SIR, the dB loss caused by CCI in SISO system is about 5.7 dB. The dB loss caused by CCI in MIMO system is 2.2 dB. The CCI has great influence to the SISO systems but also has significant influence onto MIMO system. According to these results, system with less than 5dB SIR CCI may not be acceptable to use for some communication purpose, because of its performances are highly affected.

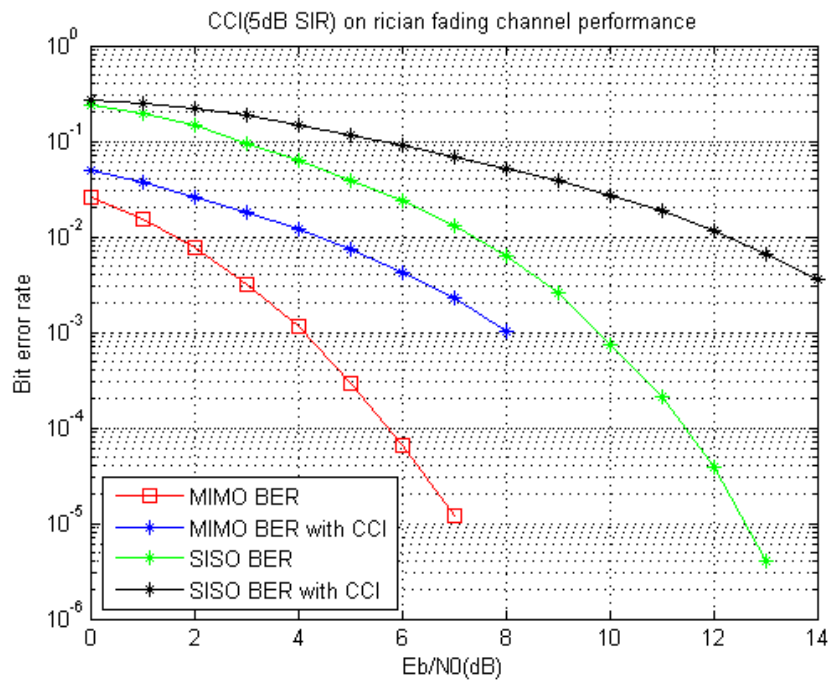
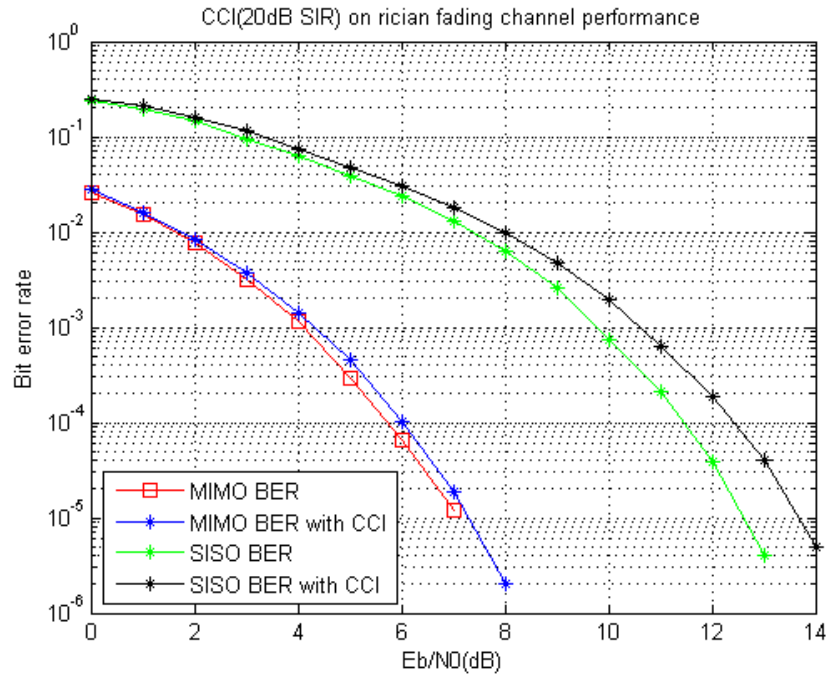


Figure 4-6 CCI BER Performance for $k = 12$ dB, $f_d = 100$ Hz

Figure 4-6 shows the Rician fading channel system with CCI BER performance where $k = 12\text{dB}$, $f_d = 100\text{Hz}$. For different SIR values, the BER performance of the system is not the same.

For 20dB SIR, the dB loss caused by CCI in SISO system is 0.2 dB. The dB loss caused by CCI in MIMO system is 0.03 dB. The CCI has certain influence to the SISO systems but almost none to the MIMO system.

For 5dB SIR, the dB loss caused by CCI in SISO system is about 4.3 dB. The dB loss caused by CCI in MIMO system is 2.3 dB. The CCI has great influence to the SISO systems but also significant influence to MIMO system.

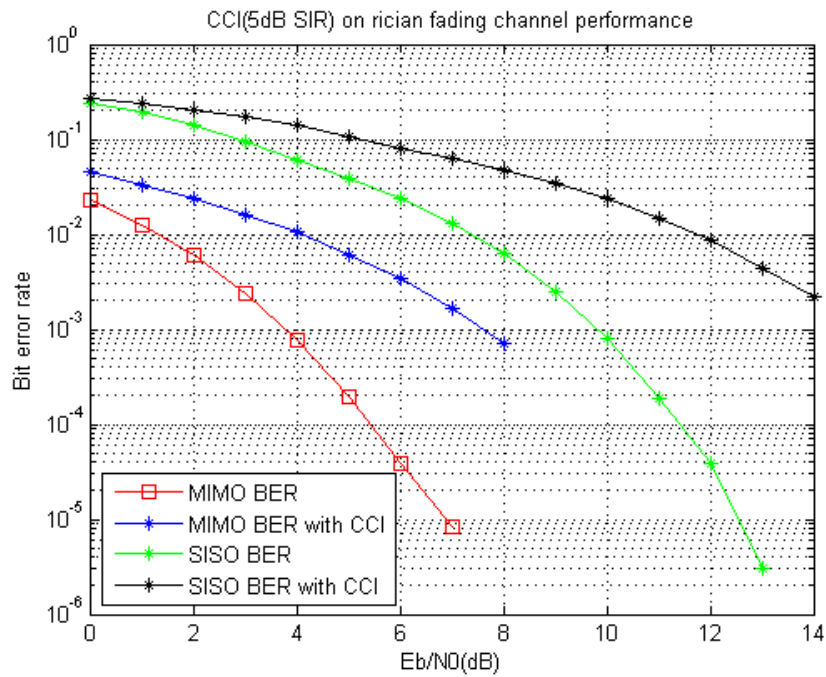
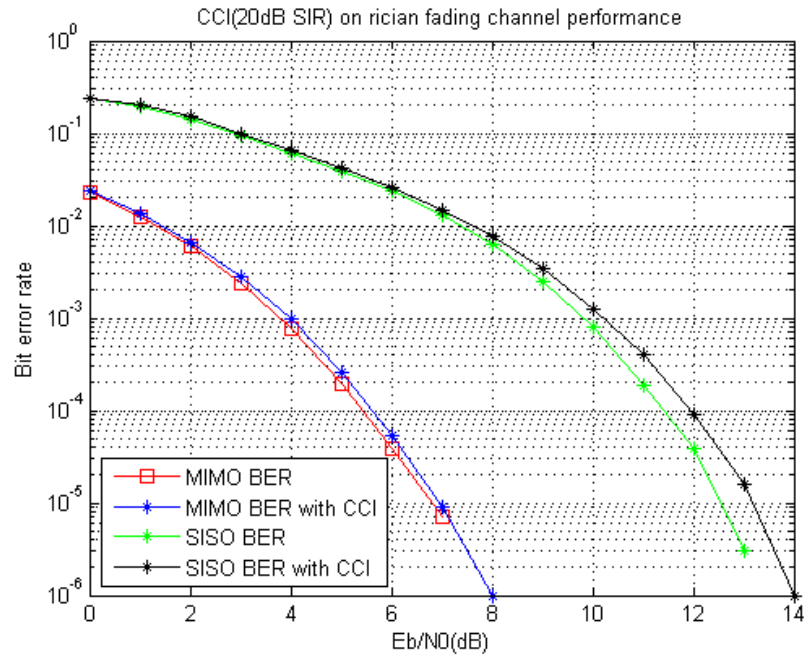


Figure 4-7 CCI BER Performance for $k = 200$ dB, $f_d = 0$ Hz

Figure 4-7 shows the Rician fading channel system with CCI BER performance where $k = 200$ dB, $f_d = 0$ Hz. The dB loss for each case is vary with different SIR values.

For 20 dB SIR, the dB loss caused by CCI in SISO system is 0.05 dB. The dB loss caused by CCI in MIMO system is 0.01dB. There is very little impact to the system by CCI of 20dB SIR, when the scatter path components are weak and the Doppler shift is 0.

For 5 dB SIR, the dB loss caused by CCI in the SISO system is about 4 dB. The dB loss caused by CCI in the MIMO system is 2.2 dB. In this case, CCI has great influence to the SISO systems but also significant influence on the MIMO system.

From the results of the BER performance of CCI with different SIR ratio, the CCI affects the accuracy of received data more as the SIR of CCI increased. The MIMO system performances are better than SISO system performance under the same effects by CCI.

Chapter 5

Combined Interference

5.1 Introduction

For the modern wireless systems, channel impairments and channel interference are among the most frequent interferences in the telecommunication world. Most of the time, interferences like these do not occur individually, but affect the system all at the same time. The combined effect of these different factors could lead to unpredictable distortions in the system. Relevant compensation schemes that apply to only one of the factors may not be able to handle the combined interferences.

The combined impact of channel impairments and channel interference has to be studied for better understanding of how these interferences behave in the real world. Also, by comparing the combined interference simulation result with the individual impairment simulation, conclusion on which factor is more dominate can be drawn.

5.2 Combined Interference System Model

In the simulation, all the interferences including DC offset, IQ imbalance, phase noise and CCI are all added to the Rician fading channel wireless system. The modulated symbols after crossing Rician fading channel are shown in figure 5-1, and the symbols with combined interference are shown in figure 5-2. The symbols with combined interference are much more scattered comparing to symbols with only one of the interferences.

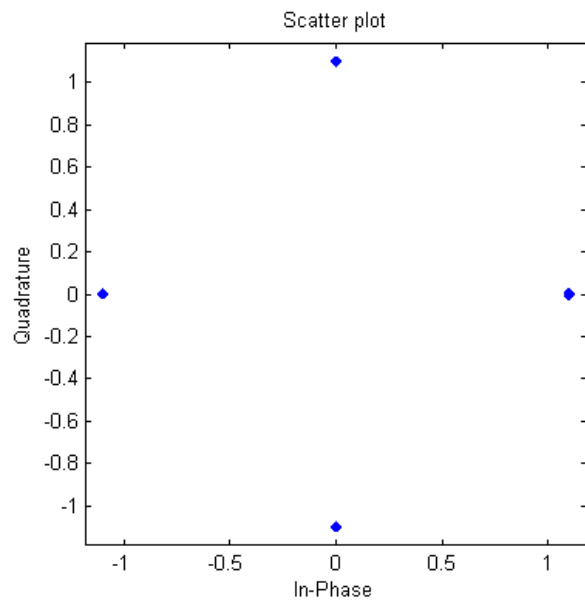


Figure 5-1 Modulated Symbol

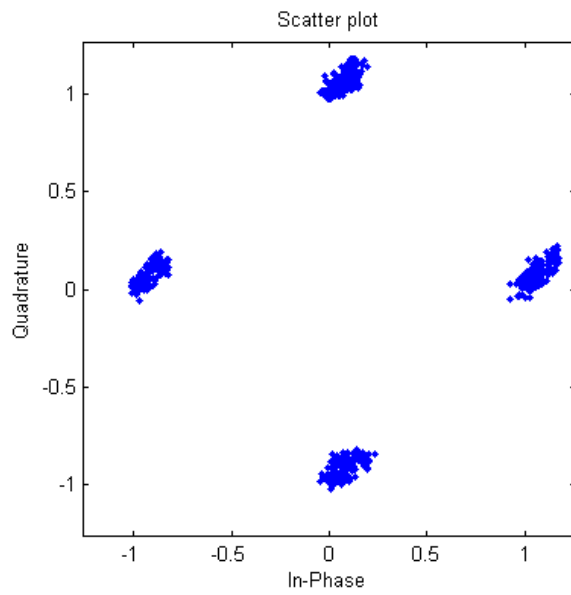


Figure 5-2 Symbols with Combine Interferences

The symbols are highly distorted after the combined effect. For DC offset and IQ imbalance, their impacts to the complex signals are fixed for each simulation trial. However, due to the randomness of phase noise interference and CCI model, their influences on received signals are vary for each simulation trial. The parameters and assumptions on the simulation of this section are the same as the previous simulations.

5.3 Combined Interference Simulation Results

The combined interference is added to the modulated signals after passing through the Rician fading channel. The SIR ratio for CCI is set to be 15 dB. The average BER performance is obtained by running the simulation one thousand times with each SNR value, with increment of 1 dB. The combined interference system BER is used to compare with the system BER with no combined interference, in order to find out the dB loss due to combined interference in the system.

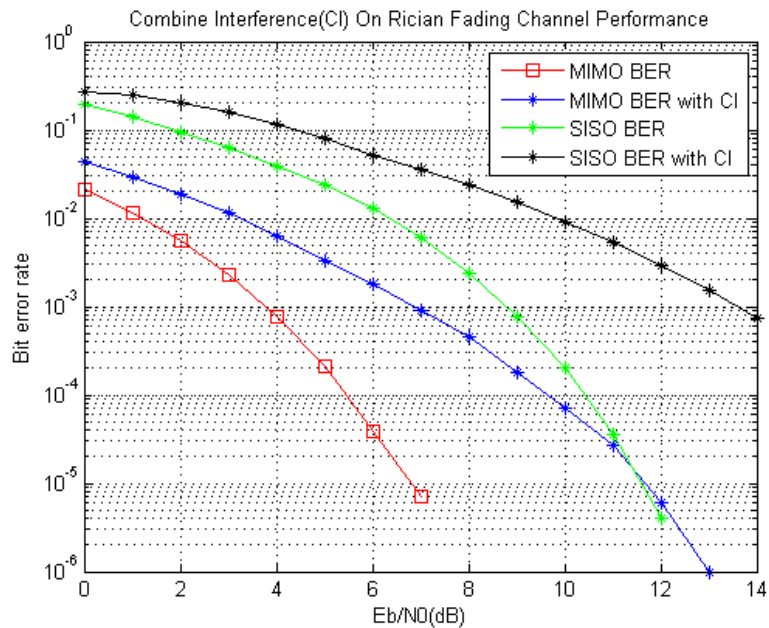


Figure 5-3 Combined Interference BER Performance for $k = 7$ dB, $f_d = 20$ Hz

For 15dB SIR CCI, with $k = 7$ dB and $f_d = 20$ Hz, the dB loss caused by combined interference in the SISO system is 2.9 dB. The dB loss caused by combined interference in a MIMO system is 1.9 dB. There is a large impact to the SISO system by combined interference. The combined interference also has a significant influence to the MIMO.

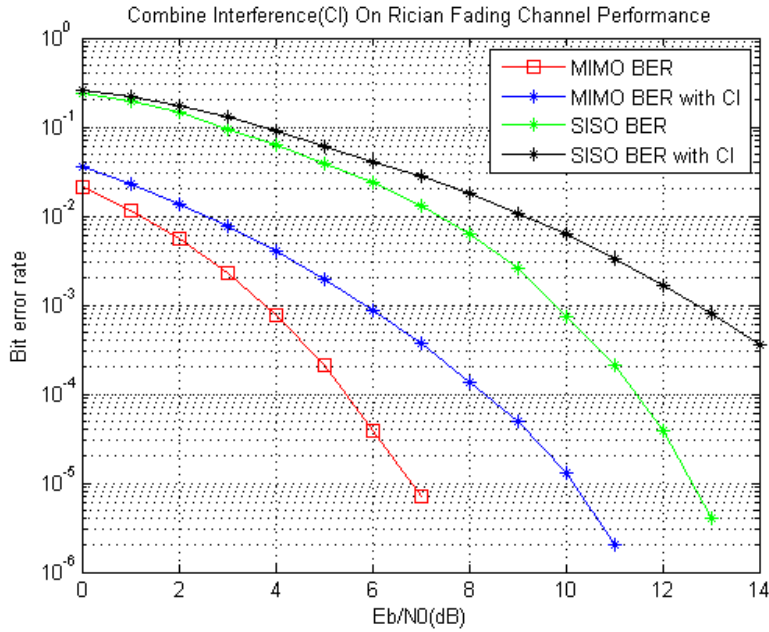


Figure 5-4 Combined Interference BER Performance for $k = 12$ dB, $f_d = 100$ Hz

For 15dB SIR, with $k = 12$ dB and $f_d = 100$ Hz, the dB loss caused by combined interference in the SISO system is 1.6 dB. The dB loss caused by combined interference in MIMO system is 1.1 dB. There is a significant impact to the SISO system by combined interference. And the MIMO system has less dB loss comparing to SISO system.

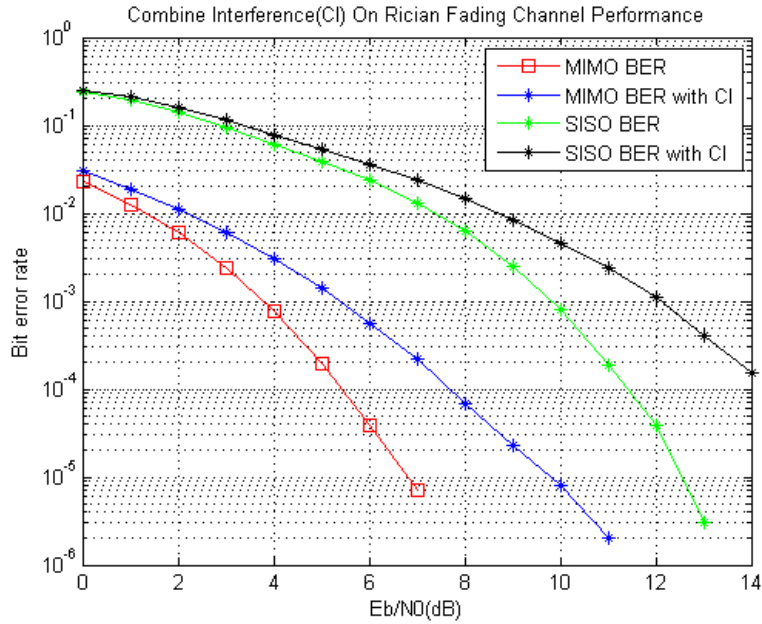


Figure 5-5 Combined Interference BER Performance for $k = 200$ dB, $f_d = 0$ Hz

For 15dB SIR, with $k = 200$ dB and $f_d = 0$ Hz, the dB loss caused by combined interference in the SISO system is 1.1 dB. The dB loss caused by combined interference in MIMO system is 0.7 dB. The combined interference impacts on both the SISO system and MIMO system are about the same.

Chapter 6

Conclusion and Future Work

6.1 Conclusion

With the rapid growth of the modern wireless system market, the impacts of channel impairments and co-channel interferences are becoming more important. Systems suffering from these interferences will experience distortions of signals and reduction of data rates. Telecommunication engineers are trying to decide how to eliminate the interferences with different compensation schemes and cancellation methods. This thesis presents the system performances under co-channel interference and channel impairments, including DC offset, IQ imbalance and phase noise. The system behaviors under different scenarios have been studied to gain a better understanding of these interferences.

All these interferences are added to the wireless model for the system that uses burst structure, QPSK modulation, Rician fading channel and block phase estimation. The interferences are all added to the system after signals passing through the Rician fading channel. The DC offset signal is constructed by starting with an element of zero value, and increase each element value continuously, until it reaches the last element with the value that is five percent of the maximum received signal value. The IQ imbalance is added to the system by shifting the received symbols phase by 5 degrees, after calculating the phase of each symbol. The phase noise interference shifts the phase of each symbol by a random value, from +10 degrees to -10 degrees. To add the CCI to the system, the SIR of CCI is defined to be either 5, 10, 15 or 20. The channel interference signal is generated by another system that has the same system design and fading channel, before adding to the current system.

Table 6-1 Summary of SISO Performance with Different Interferences

Unit: dB	k=7dB, $f_d=20\text{Hz}$	k=12dB, $f_d=200\text{Hz}$	k=200dB, $f_d=0\text{Hz}$
DC offset	1.4	0.7	0.2
IQ Imbalance	0.9	0.15	0
Phase Noise	1	1	0
CCI (20dB SIR)	1.1	0.2	0.05
CCI (15dB SIR)	1.7	0.8	0.8
CCI (10dB SIR)	3.2	2.7	1.9
CCI (5dB SIR)	5.7	4.3	4
Combined	2.9	1.6	1.1

Table 6-2 Summary of MIMO Performance with Different Interferences

Unit: dB	k=7 dB, $f_d=20\text{Hz}$	k=12dB, $f_d=200\text{Hz}$	k=200dB, $f_d=0\text{Hz}$
DC offset	0.2	0.1	0.1
IQ Imbalance	0.05	0.07	0.05
Phase Noise	0	0.5	0
CCI (20dB SIR)	0	0.03	0.01
CCI (15dB SIR)	0.3	0.3	0.3
CCI (10dB SIR)	1.0	1.2	0.9
CCI (5dB SIR)	2.3	2.3	2.2
Combined	1.9	1.1	0.7

Table 6-1 lists the amount of dB loss for the system with different k and f_d value, which k is the power ratio of the direct path and the scatter path, in dB. And f_d is the Doppler shift value in Hz.

In most scenarios, the MIMO system is much more reliable than the SISO system. In MIMO system, most dB losses caused by channel impairments and channel interferences are less than 1dB.

For DC offset interference on SISO system, the dB loss caused by the interference is quite significant for small K and large f_d . However, MIMO system performance does not suffer much from DC offset. According to the results, compensation schemes may be needed to be apply when the signal power is not much greater than the noise power.

For IQ imbalance and phase noise, their impacts to the SISO system have not exceed 1 dB loss. One of the reasons for that might be because SISO system uses block phase estimation and it takes unique words to create reference phases in order to obtain the closest phases possible to the original ones. Therefore most of the symbol phases are estimated correctly, even though they are shifted by a few degrees relative to the fading symbol phases.

For Co-channel interference, the dB loss of the system gets larger when the signal to interference power ratio decreases. For SISO system, the dB loss is greater than 1dB after SIR is smaller than 10 dB. For MIMO system, the dB loss is not so significant until the SIR reaches 5dB. There is about 2 dB losses for MIMO system when CCI has 5dB SIR value. Solutions such as adding a compensation scheme or re-planning the network need to be considered. Otherwise, CCI will significantly degraded the system performance.

For the combined interference simulations, its dB loss is slightly less than the sum of all the dB losses for each individual interference. This could be interpreted as that some of the interferences have similar impacts on the symbols. Their impacts does not add up, or some have canceled each other out. It is obvious that CCI with small SIR is more dominate on the Rician fading wireless system than the other three interferences.

Through the work of simulating different channel impairments and Co-Channel interference to Rician fading channel wireless system, each of those impacts on the system performances are clear. The tables and plots that are simulated by Matlab can support this evaluation of the channel impairments and co-channel interference on Rician fading channel. This work can help many telecommunication engineers to better plan their network and design their wireless system.

6.2 Future Work

By far, only a few of the channel impairment and co-channel interference performances are evaluated. Other interferences like frequency offset and adjacent channel interference have not been tested. Also, the assumption made in this thesis is that the wireless system uses QPSK modulation, Rician fading channel, and block phase estimator. Systems that has other modulation method, with different channels, or MIMO with different numbers of transmitter and receivers have to be studied as well. To reduce the impacts or resolve the problems with interferences, new circuit level design and new system level design are needed.

References

- [1] Goldsmith, Andrea. *Wireless communications*. Cambridge: Cambridge University Press, 2005. Print.
- [2] Rappaport, Theodore S.. *Wireless communications: principles and practice*. Upper Saddle River, N.J.: Prentice Hall PTR, 1996. Print.
- [3] Chi-Hsiao Yih, "Analysis and Compensation of DC Offset in OFDM Systems Over Frequency-Selective Rayleigh Fading Channels," *Vehicular Technology, IEEE Transactions on* , vol.58, no.7, pp.3436,3446, Sept. 2009
- [4] "Co-channel interference", http://en.wikipedia.org/wiki/Co-channel_interference.
- [5] W. C. Jakes, *Microwave Mobile Communications*. Wiley, 1974; re-issued by IEEE Press, 1994.
- [6] R. H. Clarke, "A statistical theory of mobile-radio reception," *Bell Syst. Tech. J.*, pp. 957-1000, Jul.-Aug. 1968.
- [7] "Pulse shape filtering in communication systems", <http://www.ni.com/white-paper/3876/en/>
- [8] Forouzan, Behrouz A., and Catherine Ann Coombs. *Data communications and networking*. 2nd ed. Boston: McGraw-Hill, 2001. Print.
- [9] Viterbi, A, "Nonlinear estimation of PSK-modulated carrier phase with application to burst digital transmission," *Information Theory, IEEE Transactions on* , vol.29, no.4, pp.543,551, Jul 1983
- [10] "Direct Conversion Receiver" http://en.wikipedia.org/wiki/Direct-conversion_receiver.
- [11] W. Namgoong and T. H. Meng, "Direct-conversion RF receiver design," *IEEE Trans. Commun.*, vol. 49, no. 3, pp. 518-529, Mar. 2001.
- [12] R. Svitek and S. Raman, "DC offsets in direct-conversion receivers: characterization and implications," *IEEE Microwave Mag.*, vol. 6, no.3, pp. 76-86, Sept. 2005.

- [13] T. Yuba and Y. Sanada, "Decision directed scheme for IQ imbalance compensation on OFCDM direct conversion receiver," IEICE Trans. Commun., vol. E89-E, no. 1, pp. 184-190, Jan. 2006.
- [14] C.-H. Yih, "Analysis and compensation of DC offset in OFDM systems over frequency-selective Rayleigh fading channels," IEEE Trans. Veh. Technol., vol. 58, no. 7, pp. 3436-3446, 2009.
- [15] Mamiko Inamori, Anas M. Bostamam, Yukitoshi Sanada, and Hideki Minami, "IQ Imbalance Compensation Scheme in the Presence of Frequency Offset and Dynamic DC Offset for a Direct Conversion Receiver," IEEE Trans. wireless commun., vol. 8, no. 5, pp. 2214-2220, May 2009.
- [16] G. T. Gil, I. H. Sohn, Y. H. Lee, Y. I. Song, and J. K. Park, "Joint ML estimation of carrier frequency, channel, I/Q mismatch, and DC offset in communications receivers," IEEE Trans. Veh. Technol., vol. 54, no.1, pp. 338-349, Jan. 2005.
- [17] "Phase noise basics", http://www.ieee.li/pdf/essay/phase_noise_basics.pdf
- [18] T. Pollet, M. V. Bladel, and M. Moeneclaey, "BER sensitivity of OFDM systems to carrier frequency offset and Wiener phase noise," IEEE Trans. Commun., vol. 43, no. 2/3/4, pp. 191-193, Feb./Mar./Apr. 1995.
- [19] C. Muschallik, "Influence of RF oscillators on an OFDM signal," IEEE Trans. Consum. Electron., vol. 41, no. 3, pp. 592-603, Aug. 1995.
- [20] T. S. Rappaport. wireless Communication, Englewd ms. NI: Prenticc-H~, 1996
- [21] Jiang li and Qilian Liang "Overcoming co-channel interference in TDMA systems using SOM equalizer," Radio and Wireless Conference, 2003. RAWCON '03.
- [22]"multiple-cell-mimo",<http://www.profheath.org/mimo-communication/multiple-cell-mimo/>

Biographical Information

Zhaoheng Luo received his Bachelor degrees of Electrical Engineering at University of Texas at Arlington in August 2012. He then started to pursuit his master degrees of Electrical Engineering in the fall of 2012. During the summer of 2013, he spent three months working as an intern network engineer in XO. Communications. Due to his interest in telecommunications and motivations to learn more after his internship, he started to do research under Dr. Qilian Liang in Wireless communication network lab. His interest in telecommunication includes wireless communication and software defined network.